Aus der Klinik für Gynäkologie mit

Schwerpunkt gynäkologische Onkologie

der Medizinischen Fakultät Charité-Universitätsmedizin Berlin

# DISSERTATION

## Evaluation of Cytotoxic Effects and Underlying Mechanisms of Disulfiram on Breast Cancer Cell Lines

Zur Erlangung des akademischen Grades
Doctor medicinae (Dr. med.)
vorgelegt der Medizinischen Fakultät
Charité - Universitätsmedizin Berlin
Von

ZHI YANG

aus Shanghai, China

Datum der Promotion:
07.12.2018

# CONTENTS

# ABBREVIATIONS AND ACRONYMS

| | |
|---|---|
| ALDH | Aldehyde dehydrogenase |
| BCSCs | Breast cancer stem cells |
| bFGF | Basic fibroblast growth factor |
| CSCs | Cancer stem cells |
| DEAB | Diethylaminobenzaldehyde |
| DMEM | Dulbecco's Modified Eagle's medium |
| DMSO | Dimethylsulfoxide |
| DRI | Dose-reduction index |
| DSF | Disulfiram |
| EDTA | Ethylenediaminetetraacetic acid |
| EGF | Epidermal growth factor |
| ER | Endoplasmic reticulum |
| ERs | Estrogen receptors |
| FBS | Fetal bovine serum |
| GSH | Glutathione |
| $H_2O_2$ | Hydrogen peroxide |
| HER2 | Human epidermal growth factor 2 receptor |
| HO• | Hydroxyl free radicals |
| HR+ | Hormone-receptor positive |
| MDC | Monolayer-derived cells |
| MTT | 3-(4,5-dimethylthiazol-2-yl)-2,5-diphenyltetrazolium bromide |
| NADPH | Nicotinamide Adenine Dinucleotide Phosphate Hydrogen |

| | |
|---|---|
| $O_2^{\bullet-}$ | Superoxide free radicals |
| PBS | Phosphate-buffered saline |
| PRs | Progesterone receptor |
| ROS | Reactive oxygen species |
| SDC | Spheroid-derived cells |
| SDS | Sodiumdodecylsulfate |
| TNBCs | Triple-negative breast cancers |

# Summary

**Background:** Accumulating evidence has implicated ALDH+ cancer cells that exhibit many features of cancer stem cells as a cause of metastasis and recurrence in breast cancer because of their unique characteristics, including quiescent proliferation status, self-renewal capacity and pluripotency. Disulfiram (DSF), which is an inhibitor of ALDH, is inexpensive, accessible worldwide, and an approved drug. Investigation of the inhibitory effect of DSF and combination effect of DSF/cisplatin will potentially improve the therapeutic outcomes of patients.

**Methods:** The cytotoxic effect of DSF on breast cancer cells was demonstrated by MTT assay. Spheroid formation, ALDH activity assay by FACS, and stemness-related transcription factor expression (Sox2, Oct3/4 and Nanog) by RT-PCT were performed to investigate the inhibitory effect on breast cancer stem cells. Cell sorting was used to further assess the effect of DSF on ALDH+/- cells. Cellular apoptosis, cell cycle, and intracellular reactive oxygen species (ROS) were detected by flow cytometry to further explore the mechanisms of DSF/cisplatin combination.

**Results:** Disulfiram exhibited dose-dependent cytotoxicity on breast cancer cell lines in vitro. 1 μM DSF was found to be adequate to inhibit spheroid formation. The average spheroid number decreased from 5 to 1 in MCF7, from 5 to 0 in MDA-MB-435S, and from 3 to 1 in SKB-R3 compared with untreated control cells, respectively ($P<0.05$). The mRNA levels of Sox2, Oct3/4, and Nanog of SDCs after DSF treatment were all significantly decreased, and even lower than those observed in MDCs ($P<0.05$). DSF sensitized breast cancer cells for cisplatin treatment, and induced more cellular apoptosis when combined with cisplatin. DSF overcame cisplatin resistance in ALDH+ cells and yielded a synergistic effect in combination with cisplatin ($CI<1$). DSF/cisplatin enhanced the accumulation of more ROS than by single drug treatment. DSF showed a concentration-dependent and time-dependent effect on ROS accumulation. ROS production in ALDH+/- cells reached the same level after DSF treatment.

**Conclusion:** Our findings provided strong evidence that DSF modulates ALDH activity and increases sensitivity to cisplatin treatment in breast cancer cells. Our results indicated that CSC-mediated cisplatin-resistance in breast cancer could be abrogated by DSF. Thus, DSF, as a synergistic agent, could be considered to be investigated as a novel candidate adjuvant chemotherapeutic agent combined with cisplatin in breast cancer treatment.

# Zusammenfassung

**Hintergrund:** Mit zunehmender Evidenz werden ALDH+ Tumorzellen, die viele Eigenschaften mit Tumorstammzellen (CSC) teilen, als Ursache für Metastasierung und Rezidivierung bei Brustkrebspatientinnen identifiziert; wegen ihrer einzigartigen Eigenschaften, die proliferative Quieszenz, Fähigkeit zur Selbsterneuerung und Pluripotenz einschließen. Disulfiram (DSF), ein Inhibitor der ALDH, ist preiswert, weltweit verfügbar und ein zugelassenes Medikament. Untersuchungen zu den inhibitorischen Effekten von DSF und Kombinationen von DSF/Cisplatin könnten potentiell die therapeutischen Ergebnisse für Patienten verbessern.

**Methoden:** Der zytotoxische Effekt von DSF auf Brustkrebszellen wurde mittels MTT Test gezeigt. Spheroidbildung, ALDH Aktivitätstest durch FACS Analyse und stemness-bezogene Transkriptionsfaktorexpression (Sox2, Oct3/4 und Nanog), gemessen durch RT-PCR, wurden zur Untersuchung des inhibitorischen Effekts auf Brustkrebsstammzellen durchgeführt. Zellsortierung wurde zur weiteren Bestimmung des Effekts von DSF auf ALDH+/- Zellen benutzt. Zelluläre Apoptose, Zellzyklus und intrazelluläre reaktive Sauerstoffspezies (ROS) wurden durchflusszytometrisch detektiert, um die Mechanismen von DSF/Cisplatin in Kombination zu untersuchen.

**Ergebnisse:** DSF zeigte eine dosisabhängige Zytotoxizität auf Brustkrebszellen in vitro. 1 μM DSF war ausreichend, um Spheroidbildung zu inhibieren. Die durchschnittliche Spheroidanzahl sank von 5 auf 1 in MCF7, von 5 auf 0 in MDA-MB-435S und von 3 auf 1 in SKB-R3 Zellen im Vergleich zu unbehandelten Kontrollzellen. Die mRNA Menge von Sox2, Oct3/4 und Nanog der SDCs nach DSF Behandlung waren alle signifikant reduziert und sogar niedriger als die in MDCs beobachteten ($P<0.05$). DSF sensitivierte Brustkrebszellen für Cisplatinbehandlung und induzierte mehr zelluläre Apoptose in Kombination mit Cisplatin. DSF überwand Cysplatinresistenz in ALDH+ Zellen und erreichte einen synergistischen Effekt in Kombination mit Cisplatin ($CI<1$). DSF/Cisplatin verstärkte die Ansammlung von mehr ROS als jede der Substanzbehandlungen alleine. DSF zeigte einen konzentrations- und zeitabhängigen Effekt auf ROS Akkumulation. ROS Produktion in ALDH+/- Zellen erreichte die gleiche Höhe nach DSF Behandlung.

**Schlussfolgerung:** Unsere Resultate liefern einen Beweis dafür, dass DSF die ALDH Aktivität moduliert und die Sensitivität für Cisplatin Behandlung bei Brustkrebszellen erhöht. Sie zeigen an, dass CSC-vermittelte Cisplatinresistenz in Brustkrebs durch DSF aufgehoben werden könnte. Demnach könnte DSF, als synergistisch wirkendes Medikament, für die Untersuchung als neuer Kandidat für eine adjuvante Chemotherapie in Kombination mit Cisplatin für Brustkrebstherapie in Betracht gezogen werden.

# 1. Introduction

## 1.1 breast cancer treatment

Breast cancer is reported to account for 29% of all new cancer cases and 14% of all cancer-related deaths among women worldwide [1]. It is rare among men, comprising 1% of all breast cancer diagnoses in USA and less than 0.1% of cancer-related deaths in males [2].
Although better therapeutic options and major improvements in public health and care have resulted in a dramatic reduction in mortality and a major increase in longevity, breast cancer mortality to incidence ratio is still around 0.31 [3]. The peak age of onset is around 40 to 50 years in Asian and 60-70 years in the western countries [4]. Female sex, family history, early age at menarche, later menopause, first childbirth after age of 30 years, and multiparity are all major independent risk factors [5].

Treatment for early breast cancer usually includes surgery and adjuvant treatment, involving endocrine therapy, chemotherapy, radiotherapy, and targeted therapies in appropriate patients. Surgical resection is the most effective method to remove primary tumors and metastatic lymph nodes, so surgery is the major component of breast cancer treatment. Endocrine therapy has been used in patients with hormone-receptor positive (HR+) breast cancer since 1977 [6]. Estrogen and progesterone are the primary regulators for the growth and differentiation of breast tissue. They exert their cellular effects by binding to the estrogen receptors (ERs) and progesterone receptors (PRs) and activating these receptors [7]. Breast cancer could be classified based on the presence of ER, PR, and human epidermal growth factor 2 receptor (HER2). Approximately 60% of all breast cancers express hormone receptor (HR+) [8]. The oncogene HER2 is overexpressed in around 20% of all cases and the remaining 20% are negative for the expression of ER, PR, and HER2, which are known as triple-negative breast cancers (TNBCs) [9, 10]. Endocrine therapy, such as tamoxifen, which is an antiestrogen drug, remains the first effective systemic treatment for female patients with hormone receptor-positive breast cancer [11]. However, when the disease becomes metastatic, all patients eventually develop endocrine resistance and require chemotherapy [12], which mainly includes cytotoxic agents, such as taxanes and cisplatin. In addition, according to the International Expert Consensus on the primary breast cancer treatment, radiation therapy is indicated in patients with four or more positive nodes to reduce the risk of local breast recurrence. However, in older patients and patients with substantial comorbidity following breast conserving surgery, radiation therapy should be avoided [13]. Patients with TNBCs tend to display an aggressive phenotype. There are

no standard targeted therapies to treat their disease, and only a limited amount of cytotoxic agents is available [14].

## 1.2 Chemotherapy resistance in breast cancer

Numerous chemotherapeutic drugs have been approved as adjuvant treatment of all breast cancer subtypes including TNBCs. Unfortunately, response rates for first-line chemotherapies are approximately 30%-70% [15], and most patients treated with these drugs eventually develop resistance, often leading to enhanced disease progression and poor prognosis.

Drug resistance is a major factor for the failure of chemotherapy treatment. Resistance can be manifested as a result of decreased drug activity. Resistance to chemotherapy can be primary or acquired. Primary drug resistance occurs prior to drug exposure, with tumor insensitivity to initial treatment. Acquired drug resistance occurs during or after the course of therapy. Empirically, the time to relapse after initial chemotherapy is counted in 6-month blocks. When the disease-free interval time is less than 6 months or even between 6-12 months, intrinsic or acquired drug resistance appears to be the culprit behind tumor progression [16].

A number of mechanisms are thought to be involved in the development of tumor chemotherapy resistance, including increased activity of drug efflux pumps or reduced drug influx pumps; activation of mechanisms that repair drug-induced DNA damage; activation of detoxifying proteins; and disruptions in apoptotic signaling pathways [17]. Thus, there is a significant need for new agents that are not susceptible to common tumor-resistance mechanisms, to overcome chemotherapy resistance in breast cancer.

## 1.3 Breast CSCs

The cancer stem cells (CSCs) hypothesis was first proposed for human leukemia based on the observation that a small fraction of cells could generate leukemia in severe combined immune-deficient mice, while the majority of tumor cells failed to engraft [18]. This small population of cells, termed cancer stem cells (CSCs), retain the ability to self-renew and differentiate to repopulate the entire tumor. Studies have suggested that they are responsible for tumor initiation, growth, recurrence, and for resistance to chemotherapy and radiation therapy [19,20].

The concept of breast cancer stem cells (BCSCs) proposes they arise from either mammary stem cells or progenitor cells [21,22]. Much supporting evidence shows similar phenotypic features and cell surface markers which are related to those specific cells originating from the same lineage in the differentiation hierarchy [23]. The population of BCSCs shares specific properties highly similar to normal mammary stem cells or partially differentiated mammary progenitor cells [24]. They have the ability to undergo self-renewal and differentiation, giving rise to non-tumorigenic progeny that makes up the bulk of the tumor, resistance to conventional therapy which leads to generation of more CSCs and tumor relapse. Muhammad Al-Hajj et al. prospectively identified and isolated the tumorigenic cells from the non-tumorigenic cancer cells from eight of nine patients based on cell surface marker expression. As few as 100 cells with CD44+CD24−/lowLineage− were able to form tumors in mice, whereas tens of thousands of cells with alternate phenotypes failed to form tumors. Furthermore, the tumorigenic subpopulation could be serially passaged: each time cells within this phenotype generated additional CD44+CD24−/lowLineage− tumorigenic cells, as well as the mixed populations of non-tumorigenic cells present in the initial tumor with diverse phenotypic features [25].
The discovery of stem cells in breast cancer has a great impact on cancer biology research and cancer drug discovery. As current chemotherapeutic agents may not completely eliminate CSCs, there is a need for novel compounds targeting breast CSCs to treat breast cancer and control recurrence and metastasis.

## 1.4 BCSC markers and ALDH1

A series of BCSC markers were identified to define the BCSC subpopulation, including CD44, CD24, CD166, CD47, CD133, EpCAM, and ALDH1 [26]. It was validated that the BCSCs isolated from cell lines and primary tumors by these specific markers were able to reconstitute the parent tumors in xenografts [27]. These markers are helpful in identifying characteristics of cells. Among these markers, the CD44+/CD24−/low phenotype, which was first documented in 2003, is a commonly used marker to characterize BCSCs [25]. CD44 is a cell surface adhesion molecule that mediates cell-cell and cell-extracellular matrix (ECM) interactions, whereas CD24 is a small glycoprotein involved in negatively regulating the activity of chemokine receptor CXCR4, which can mediate breast cancer metastasis [27]. Therefore, breast cancer cells with increased CD44 expression and decreased CD24 expression should possess an effective ability to induce malignant progression. However, there is a debate over the relationship between CD44+/CD24−/low phenotype and tumorigenicity. Experiments showed that

CD44+/CD24− cells could not always form tumor cells [28]. In another study, patients with CD44−/CD24+ status, rather than CD44+/CD24−, were identified with worse prognosis in breast cancer [29].

The controversy of CD44+/CD24− cells calls for better BCSC markers. ALDH1 has come to the forefront as a BCSC marker. ALDH1 play important roles in retinoid signaling, acetaldehyde metabolism, and reactive oxygen species (ROS). ALDH1 activity can be assessed by the ADELFLUOR assay. An ALDEFLUOR-positive subpopulation isolated from human breast tumors was highly enriched in tumorigenic capacity [30]. Tumor cells with higher ALDH1 activity have also been reported with increased capacity to form spheroids in breast cancer [31]. In addition, ALDH1 positive cells display stem-like behavior such as differentiation, tumor cell self-protection, expansion, and chemotherapy resistance [32]. Given the capacity of BCSCs to generate bulk primary tumor, it is expected that novel, potent and ALDH1-specific inhibitors could enter experimental and clinical assessment in breast cancer therapy in coming years. This suggests that the combination of ALDH1-specific targeted agents and individualized therapies of breast cancer may be more effective therapeutic strategies in breast cancer and improve the clinical outcome.

## 1.5 Anti-cancer activity of Disulfiram

Disulfiram (DSF), a member of the dithiocarbamate family, has been a FDA-approved drug in clinical treatment of alcohol dependence for over 60 years. Initially, the compound had been used in the process of rubber manufacturing. In 1937, workers who were regularly exposed to DSF exhibited flu-like symptoms when they ingested alcohol [33]. DSF was approved for short-term and long-term treatment of alcoholism under physician supervision since 1948 [34].

Over the past years, however, increasing evidence indicates that DSF possesses a great potential for the treatment of human cancers. DSF's anticancer activity has been demonstrated in various cancer types [35-38]. It has been proven that DSF reacts with redox-sensitive sulfhydryl groups (thiols) which are characterized by the presence of sulfhydryl groups (-SH) at their active center, to further contribute to antioxidant defense mechanisms [39, 40]. ALDH enzymes contain sulfhydryl groups. Thus, the key of DSF's anticancer action relates to its ability to target aldehyde dehydrogenase (ALDH), and inhibit proteasome activity in cancer cells by forming complexes with metal ions. Considering that the pharmacokinetics of DSF is well-established

and a safety profile has been verified for decades, this agent is an attractive “old” drug that has great potential for novel developments in breast cancer treatment [41]. However, the mechanisms of DSF action on cancer stem cells have not been fully explained. In addition, DSF may also support current chemotherapy that is in dire need of novel treatments that could reduce adverse side effects due to high drug doses. Therefore, further investigations are needed to establish dosing schedules and chemotherapeutic combinations which will generate the greatest response in breast tumor cells.

## 1.6 Drug combination

Ever since the earliest days of recorded medical history, drug combinations have been used for treating diseases and reducing suffering. During the past century, attempts have been made to quantitatively measure the dose-effect relationships of each drug alone and its combinations and to determine whether or not a given drug combination would gain a synergistic effect [42]. These applications are most noticeable in the areas of anti-cancer drug research. In drug combinations, different drugs may target on different targets, or different cell subpopulations simultaneously. Drugs with different mechanisms could also be combined to enhance the effect of single drugs and to treat cancer cells more effectively [43, 44].

There are several possible favorable outcomes for drug combinations. Firstly, the efficacy of the therapeutic effect could be increased in combinations. Secondly, the dosage of each drug in combinations could be decreased to reduce toxicity, while increasing or at least maintaining the same efficacy. Thirdly, selective synergism or efficacy synergism could be provided against target during drug combination. Fourthly, the development of drug resistance in patients could be minimized or slowed down [43, 44]. For these therapeutic benefits, drug combinations have been widely used and became the leading choice for treating cancers.

## 1.7 ROS in cancer cells and in CSCs

Reactive oxygen species (ROS) are broadly defined as oxygen-containing chemical species with reactive properties, including the superoxide ($O_2$•−) and hydroxyl (HO•) free radicals as well as non-radical molecules such as hydrogen peroxide ($H_2O_2$) [45]. In biological systems, cellular metabolism is balanced by ROS generation systems and ROS elimination systems to maintain a stable redox state for ensuring cell survival and functions. ROS generation systems include the

mitochondrial respiratory chain, the endoplasmic reticulum (ER), and hypoxia and so on [45-47]. ROS scavenging systems are mainly glutathione (GSH) and Nicotinamide Adenine Dinucleotide Phosphate Hydrogen (NADPH), and tumor suppressor genes and ALDH [48-50]. Once this balance is destroyed, excess amount of ROS causes oxidative damage of lipids, nucleic acids, and amino acids which will lead to cellular dysfunction and death [51].

Cancer cells have a high demand for ATP due to rapid growth and limited availability of nutrients, and thus have large consumption of oxygen, and high levels of oxidative stress, resulting in the accumulation of ROS. Many types of cancer cells have been proven with increased levels of ROS compared with their normal counterparts [52,53]. A diversity of mechanisms is involved in this ROS increase in cancer cells, including mitochondrial dysfunction, aberrant metabolism, the activation of oncogenes, and inflammatory cytokines and others [54-57].

CSCs are hypothesized to have low levels of intracellular ROS compared with cancer cells. Experiments have shown that CD44+CD24-/lowLin- BCSC-enriched populations contain significantly lower levels of ROS than their non-tumorigenic progeny [58]. Since cancer cells with increased levels of ROS are likely to be more vulnerable to further ROS increase, lower levels of ROS in CSCs would protect them from endogenous and exogenous ROS-mediated damage, and maintain their functions such as radiotherapy and chemotherapy resistance. Lower ROS levels in CSCs are usually associated with increased expression of scavenger, including GSH and ALDH which could protect CSCs against oxidative stress induced by alcohol, UV radiation, and some chemotherapeutic agents.

# 2 Aim of the study

The objective of this thesis was to investigate the inhibitory effect of DSF on breast cancer cells, the combination effect of DSF/cisplatin, and the possible mechanisms for the enhanced toxicity of this combination. Therefore, the following aims were pursued:

1. To investigate the inhibitory effect of DSF on breast cancer stem cells.

2. To assess the potential synergism of DSF in combination with cisplatin in breast cancer cell lines.

3. To investigate the effect of DSF on CSC-mediated cisplatin-resistant cells.

4. To explore the potential cytotoxicity mechanisms for DSF/cisplatin combination in vitro by cell cycle and ROS analysis.

# 3 Materials

## 3.1 Laboratory Equipment and Materials

| | |
|---|---|
| Axiovert 40 CFL | Carl Zeiss, Jena, Germany |
| BD FACSCalibur System | BD Bioscience, Heidelberg, Germany |
| Freezer, -80°C | Heraeus, Hanau, Germany |
| Incubator, HERA cell 150 | Heraeus, Hanau, Germany |
| Multicentrifuge | Heraeus, Hanau, Germany |
| Nanodrop | Peqlab, Erlangen, Germany |
| Pipettes | Eppendorf AG, Hamburg, Germany |
| Smart SpecTM Plus Spectrophotometer | BioRad, München, Germany |
| Thermocycler | Eppendorf AG, Hamburg, Germany |
| Vortexer | Scientific Industries, N.Y., USA |
| BD Falcon™ Cell Culture Flasks | BD Bioscience, Franklin Lakes, USA |
| BD Falcon™ Propylene Conical Tubes | BD Bioscience, Franklin Lakes, USA |
| BD Falcon™ Tissue Culture Dish (100*200mm) | BD Bioscience, Franklin Lakes, USA |
| Cell Culture Plates (6-, 24-, 96-well) | BD Bioscience, Franklin Lakes, USA |
| Ultra-Low Attachment Cell Culture Plate | Corning, NY, USA |
| 40 µm Cell strainer | Corning, NY, USA |
| BD FACSAriaII SORP | BD Bioscience, Heidelberg, Germany |
| Multiskan FC Microplate Photometer | Thermo Scientific, MA, USA |

## 3.2 Chemicals and Reagents

| | |
|---|---|
| Agarose | Biozym, Oldendorf, Germany |
| BD FACSflow™ | BD Sciences, Franklin Lakes, USA |
| Chloroform | Biochrom, Berlin, Germany |
| Dimethylsulphoxide (DMSO) | Sigma-Aldrich, Deisenhofen, Germany |
| Ethanol, 70% | Biochrom, Berlin, Germany |
| Epidermal Growth Factor (EGF) | Biochrom, Berlin, Germany |
| Fetal bovine serum (FBS) | Gibco BRL, Karlsruhe, Germany |
| Fibroblast Growth Factor-basic (bFGF) | Biochrom, Berlin, Germany |
| Isopropanol | Biochrom, Berlin, Germany |

| | |
|---|---|
| Penicillin/Streptomycin | Biochrom, Berlin, Germany |
| Phosphate-buffered saline (PBS) without $Mg^{2+}/Ca^{2+}$ | Biochrom, Berlin, Germany |
| Trypsin/EDTA Solution | Biochrom, Berlin, Germany |
| TRIzol reagent | Sigma-Aldrich, Deisenhofen, Germany |

## 3.3 Cell Culture Media and Kits

| | |
|---|---|
| Dulbecco's modified Eagle's Medium with GlutaMAX™-I (DMEM) | Invitrogen, Heidelberg, Germany |
| Quantum 263 medium | PAA, Cölbe, Germany |
| RPMI 1640 | Invitrogen, Heidelberg, Germany |
| | |
| ALDEFLUOR assay Kit | StemCell Technologies, Köln, Germany |
| FLUOS-conjugated annexin-V and Propidium iodide Kit | Roche, Mannheim, Germany |
| Mitosox Red Kit | Thermo Fisher Scientific, MA, USA |
| Power SYBR Green Master Mix | Thermo Fisher Scientific, MA, USA |
| High-Capacity cDNA Reverse Transcription Kit | Thermo Fisher Scientific, MA, USA |
| Cell Proliferation Kit I (MTT) | Roche, Mannheim, Germany |

# 4 Methods

## 4.1 Cell lines and drugs

The breast cancer cell lines MCF-7, SKB-R3 and MDA-MB-435S were cultured in DMEM medium with L-glutamine supplemented with 10% fetal bovine serum (heat-inactivated at 56°C for 30 min) and 1% penicillin/streptomycin in a humidified incubator at 37°C and 5% $CO_2$. All of our experiments were performed on cultures that were 70% confluent. Free DSF was dissolved in dimethylsulfoxide (DMSO) at a stock concentration of 10 mM, stored at −20°C. Cisplatin was kept at a stock concentration of 3.3 mM at room temperature. All drugs were diluted into working concentrations in corresponding cell culture medium before use.

## 4.2 MTT assay

Adherent monolayer cells were first expanded in 75 $cm^2$ culture flasks in standard medium until 70% confluency. Cells were washed twice with PBS without $Ca^{2+}$/$Mg^{2+}$ and detached using 3 ml Trypsin/EDTA for around 5 minutes until all the cells were detached. The reaction was stopped by addition of 2 ml of complete culture medium. The solution was poured into a 15 ml Falcon tube and centrifuged at 1500 rpm for 5 min. Cells were washed again twice with PBS without $Ca^{2+}$/$Mg^{2+}$, followed by resuspension in DMEM medium and diluted at a concentration of $4\times10^4$ cells/ml. Then a single-cell suspension was prepared.

Cells were seeded in 96-well plates at a density of 3000 cells per well in 100 µl drug-free medium and incubated overnight. Serial dilutions of DSF or cisplatin working concentrations were prepared with cell culture medium. Cell culture medium in 96-well plate was removed gently and 100 µl fresh medium with various drug concentrations was added. Each drug concentration was in triplicate. Cells without any drug treatment were used as controls. The 96-well plate was placed in the cell culture incubator for 72 h. After 72 h incubation, 10 µl of MTT labeling reagent (Cell Proliferation Kit I (MTT)) was added to each well, including controls, and the 96-well plate was then incubated at 37°C for 4 h. When the purple precipitate was clearly visible under the microscope after 4 h incubation, 100 µl solubilizition solution (Cell Proliferation Kit I (MTT)) was added to all wells, including controls, and mixed gently, incubated at 37°C overnight.

The solution absorbance was measured at a wavelength of 590 nm using a Multiskan FC Microplate Photometer (Thermo Scientific). Cellular relative viability was calculated as the

percentage of drug-treated cells from drug-free control cells. All experiments were performed in triplicate. Dose response curves and $IC_{50}$ were calculated using GraphPad Prism 5.04.

## 4.3 Spheroid formation assay

First, an ultra-low attachment plate had to be prepared. Agarose was dissolved in PBS at a concentration of 1.5% (w/v). Then, 8 ml of 1.5% agarose was filled into a 75 $cm^2$ cell culture plate. The plate was gently swirled to make sure that all the agarose covered the inner bottom of the plate entirely without any bubbles. Agarose was allowed to solidify and cool down to room temperature for 20 minutes. An ultra-low attachment plate was prepared.

Then, a single-cell suspension was prepared as described above and diluted at a concentration of $5\times10^3$ cells/ml in serum-free Quantum 263 medium, supplemented with 10ng/ml EGF and 10 ng/ml b-FGF. 10-12 ml of the cell suspension was transferred into ultra-low attachment cell culture plates. The plates were incubated in a cell culture incubator with 5% $CO_2$ at 37°C. Half of the medium was replaced every 3 days. Movement of the plates was minimized, particularly during spheroid initiation. Cells were allowed to grow for 5-8 days to form spheroids.

## 4.4 Spheroid formation inhibitory assay

To get spheroid-derived cells (SDCs), all spheroids were collected into a 40 μm cell strainer (Corning). They were then washed into a 50 ml Falcon tube with PBS, and centrifuged at 1500 rpm for 5 min. Medium was aspirated and spheroids were dissociated into single cells using 500 μl tryspin/EDTA at 37°C and 5% $CO_2$ for 5 min, followed by washing with PBS twice. Single cells were filtered through a 40 μm cell strainer and re-seeded into a 96-well ultra-low attachment plate at a density of 100 cells or 200 cells in 100 μl serum-free Quantum 263 medium per well (100 cells per well for MCF-7 and SKB-R3 cell lines; 200 cells per well for MDA-MB-435S cell line). Cells were exposed to DSF (1 μM or 5 μM) and cultured for 10 days. Cells without DSF exposure were used as controls. Spheroids with 100 μm or more in diameter were counted and photographed at 50-fold* magnification after 10 days in cell culture.

## 4.5 Flow cytometric analysis of ALDH activity and cell sorting

ALDH activity was measured by quantifying the ALDH-mediated intracellular retention of fluorescent compound BODIPY-aminoacetate (BAA-) using flow cytometry-based methods. Briefly, spheroids were collected with a 40 μm cell strainer, disaggregated into single cells by

Trypsin/EDTA digestion, and diluted into a single cell suspension ($4*10^4$/ml). All the single cells were incubated with ALDH substrate BAAA for 30 min at 37°C following the manufacturer's instructions of ALDEFLUOR assay Kit. Tested cells were exposed to DSF (10 μM). Cells treated with diethylaminobenzaldehyde (DEAB) which is a specific ALDH inhibitor, were used as controls to establish the baseline fluorescence and define the cut-off threshold for ALDEFLUOR-positive cells.

For FACS sorting, SDCs were suspended in PBS buffer at a concentration of $1\times10^7$ cells/ml and sorted on an BD FACSAria II SORP cell sorter (BD Biosciences). The sorted cells were treated with DSF or cisplatin, and relative cellular viability was done by MTT. The sorting gates were established with negative controls which were treated with DEAB.

## 4.6 Flow cytometric analysis of the cell cycle

Cells were seeded in 24-well plates at a density of $3\times10^4$ cells in 1 ml medium per well. After overnight incubation, cells were treated by indicated concentration of DSF, or cisplatin, or DSF/cisplatin combination for 72 h. Each concentration was in triplicate. Cells without treatment were used as controls. All the cells were harvested after 72 h treatment and a single cell suspension was prepared as described above.

Cells were washed twice with PBS, re-suspended in 100 μl PBS, and fixed by addition of 900 μl 70% ethanol at 4°C overnight. Cells were washed twice with PBS and centrifuged at 3000 rpm for 5 min. The cells were then incubated with RNaseA and propidium iodide for 30 min in the dark at room temperature. The final concentration was 100 μg/ml for RNaseA and 50 μg/ml for propidium iodide.

Analysis of cell cycle distribution was performed using flow cytometric analysis of DNA staining. The data from 10000 cells for each sample were collected by FACS Scan and DNA content and cell cycle was analyzed. FlowJo software (Treestar, Ashland, OR, USA) was used to quantitate the percentage of cells in each cell cycle phase.

## 4.7 Flow cytometric analysis of cellular apoptosis

Cells were cultured and treated at the indicated concentration of DSF, or cisplatin, or DSF/cisplatin combination as described above. The Annexin-V-FLUOS labelling solution was

prepared following the manufacturer's instructions of the FLUOS-conjugated annexin-V and propidium iodide Kit (Roche). Cells were washed with PBS twice and re-suspended in 100 µl of Annexin-V-FLUOS labelling solution at a density of $1\times10^6$ cells/ml. Cells were incubated in the dark at room temperature for 15 min.

Apoptosis and necrosis were evaluated using FL3 (PI) and FL1 (Annexin-V) by FACS analysis. The percentage of cells was determined in four quadrants: live cells, (Annexin-V−/PI-, lower/lower/left quadrant); early apoptotic cells (Annexin-V+/PI−, lower/right quadrant); late apoptotic cells (Annexin-V+/PI+, upper/right quadrant); and necrotic cells (Annexin-V−/PI+, upper/left quadrant), respectively.

## 4.8 RNA extraction

For monolayer: Medium was removed from culture dish. 1 ml of TRIzol reagent was added directly to the cells per 10 $cm^2$ of culture dish surface area. The cells were lysed directly in the culture dish by pipetting up and down several times. The lysed cells were transferred into a new Eppendorf tube. For spheroids: The cells were harvested by 40 µm cell strainer. Cells were centrifuged at 1500 rpm for 5 min after cell counting. The supernatant was removed and 1 ml of TRIzol was added per $10^6$ cells. The cells were lysed by pipetting up and down several times before being transferred into an Eppendorf tube.

Total RNA was extracted using TRIzol Reagent following the protocol below. Chloroform (0.2 ml per 1 ml of TRIzol reagent) was added. The tube was shaken vigorously by hand for 15 seconds and incubated on ice for 15 min. The tube was centrifuged at 12000 rpm for 15 min at 4°C. Then the mixture was separated into 3 phases: the lower organic phase containing protein; an interphase containing DNA; and the upper aqueous phase containing RNA. The upper aqueous phase was carefully transferred to a new clean tube. 0.5 ml of isopropanol was added into the new tube with the aqueous phase per 1 ml of TRIzol used. The mixture was mixed gently by inverting the tube and incubated on ice for 10 min. The tube was centrifuged at 12000 rpm for 10 min at 4°C. The supernatant was removed and the RNA pellet in the tube was washed with 1 ml 75% ethanol per 1 ml of TRIzol used in the sample preparation. The sample in the tube was mixed gently by inverting the tube a few times. The tube was centrifuged at 14000 rpm at 4°C for 5 min, and the supernatant was removed. The RNA pellet was air-dried for 10-15 min, and resuspended in DEPC-treated water.

## 4.9 Reverse transcription and quantitative real-time PCR

Total RNA (1 μg) was converted to cDNA by RT-PCR following the manufacturer's instructions of a High-Capacity cDNA Reverse Transcription Kit (Thermo Fisher Scientific). qRT-PCR was carried out using Power SYBR Green Master mix (Thermo Fisher Scientific) and run on a StepOne System (Thermo Fisher Scientific). PCR conditions were as follows: 95°C for 15 min, 40 cycles of 95°C for 2 min, 95°C for 15 sec and 72°C for 1 min. Stemness-related nuclear transcription factor mRNA of Sox2, Oct3/4, and Nanog were determined in the present study. Reactions were carried out in triplicate with RT controls. GAPDH was used as a reference gene. Data were analyzed using the modified delta-delta Ct method.

Primer sequences for Oct3/4, Sox2, and Nanog were as follows:

Oct3/4 FWD: 5'-GACAGGGGGAGGGGAGGAGCTAGG-3'
REV: 5'-CTTCCCTCCAACCAGTTGCCCCAAAC-3'
Sox2 FWD: 5'- GGGAAATGGGAGGGGTGCAAAAGAGG-3'
REV: 5'-TTGCGTGAGTGTGGATGGGATTGGTG-3'
Nanog FWD: 5'-AATACCTCAGCCTCCAGCAGATG-3'
REV: 5'-TGCGTCACACCATTGCTATTCTTC-3'

## 4.10 DSF/cisplatin combination treatment

To explore the combination effect of DSF and cisplatin which is the first-line anti-tumor drug, breast cancer cells were treated with DSF alone, or cisplatin alone, or DSF/cisplatin combination for 72 h in 96-well plates. The range of dosage of each drug was selected to cover the concentrations below and above the $IC_{50}$ values. The combination ratio was designed at a constant ratio of approximately $IC_{50}$ concentration for each drug, so that the contribution of the effect by each drug to the combination would be equal [43,44].

After 72 h of treatment, cells were all subjected to MTT assay. Quantitative analysis was performed to determine synergism or antagonism in the combination which is based on CompuSyn software of Chou and Martin [43,44]. CI $<$ 1, $=$1, and $>$1 indicate synergism, additive effect, and antagonism, respectively. CI $<$ 0.1, CI 0.1-0.3, CI 0.3-0.7, CI 0.7-0.85, CI 0.85-0.9 and CI 0.90-1.10 indicate very strong synergism, strong synergism, synergism, moderate synergism, slight synergism, and nearly additive effects. Dose-reduction index (DRI)

values is a measure of how many fold the dose of each drug in a synergistic combination may be reduced at a given effect level when compared with the doses of each drug alone [8].

## 4.11 Flow cytometric of analysis of ROS

Mitochondrial ROS were measured following the manufacturer's instructions of MitoSOX Red kit (Thermo Fisher Scientific). Briefly, cells ($3 \times 10^4$ cells/well) were seeded in a 24-well attachment plate and incubated overnight. After 24 h plating, cells were treated with the indicated drug for 30 min at 37°C. All the cells were harvested and washed twice with warm PBS. MitoSOX Red Reagent was prepared at a final working concentration of 5 μM with fresh medium. Cells were incubated with MitoSOX Red Reagent for 15 minutes at 37°C, and then washed gently three times with warm buffer. Mean fluorescence intensity was determined by flow cytometry. Samples without MitoSOX Red Reagent were used as the background. Samples treated with MitoSOX Red Reagent, but without any drug treatment, were used as controls. Mean fluorescence intensity was determined and all samples were normalized to untreated control samples.

# 5 Results

## 5.1 Disulfiram exhibits dose-dependent cytotoxicity on breast cancer cell lines in vitro

To explore the inhibitory effect of DSF in vitro, we initially examined the cytotoxicity of DSF on three breast cancer cell lines by MTT assay. As shown in Figure 1, no significant cytotoxicity (percentage of cytotoxicity ＞ 20%) was observed when cells were exposed to 0.04 μM, 0.2 μM, 1 μM, or 5 μM DSF in MDA-MB-435S and SKB-R3 cell lines. In MCF-7 cell line, DSF showed slight cytotoxicity at the concentration of 0.04 μM, 0.2 μM, or 1 μM, and a moderate cytotoxicity at a 5 μM concentration. However, there was a significant decrease in cellular relative viability when the concentration of DSF was increased to 25 μM. The results indicated that DSF exhibited its cytotoxicity on the investigated breast cancer cell lines in a dose-dependent manner and at higher concentrations. For further exploration of the inhibitory effects on spheroid formation and the expression of stemness-related markers in the following experiments, the concentration of DSF was chosen at concentrations lower than 5 μM which per se did not kill many cells investigated during the observation period.

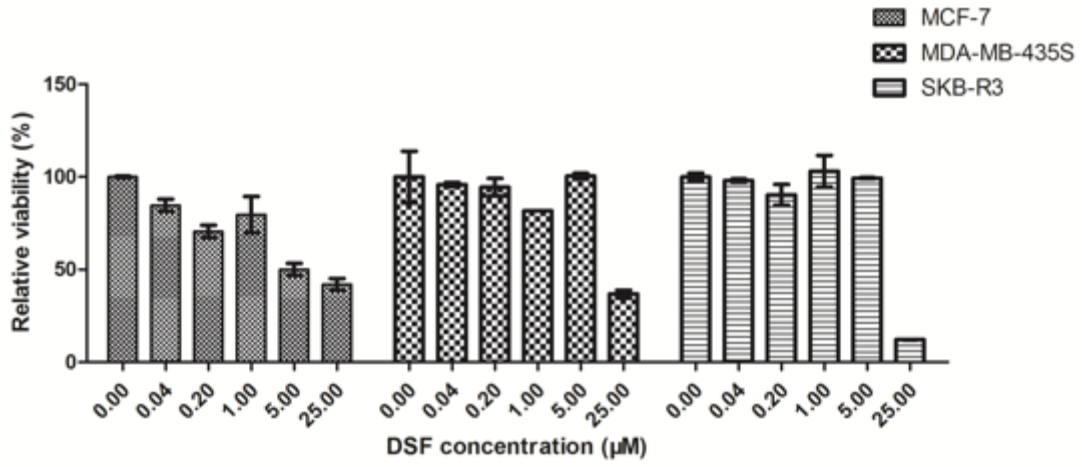


**Figure 1: Cytotoxicity of DSF on breast cancer cell lines.** MCF-7, MDA-MB-435S, and SKB-R3 cells were treated with different concentrations (0.04 μM – 25 μM) of DSF for 72 h. Cellular viability was analyzed by MTT assay. Results are mean ± SD (n = 3) of one representative experiment out of three.

## 5.2 DSF inhibits spheroid formation in breast cancer cell lines

Spheroid formation assay is a well-accepted assay to enrich for cells exhibiting positivity for established stem cell markers. The outgrowth of spheroids from anchorage dependent cell lines and their size reflects the proliferative potential of stem cells.

In order to study the inhibitory effect of chemical compounds and their combinations, the concentration used should not be cytotoxic per se. According to Figure 1, we chose a DSF concentration of 1 μM or 5 μM, and observed the ability of breast cancer cell lines to from spheroids. Spheroid-derived cells were treated with 1 μM or 5 μM DSF in a 96-well ultra-low attachment plate (100 cells in 0.2 ml medium/well) for 7-10 days and photographed at 50 × magnification. Cells without drug treatment were used as controls. Spheroids were counted in when the diameter of spheroids was more than 100 μm.

As shown in Figure 2A and Figure 2B, 1 μM and 5 μM of DSF were found to be adequate to inhibit spheroid formation while avoiding too much cytotoxicity on cellular growth. The results showed that the number of spheroids significantly decreased when cells were exposed to 1 μM DSF (the average spheroid number decreased from 5 to 1 in MCF7, from 5 to 0 in MDA-MB-435S, and from 3 to 1 in SKB-R3). In addition, the individual size of the forming spheroids was also was reduced in all cell lines not reaching the cut off of 100 μM. No growth of spheroids was observed when the cells were exposed to 5 μM DSF in any of the three cell lines investigated. This demonstrated that at this concentration, despite very low direct toxicity, a stemness inhibitory effect could be achieved.

A

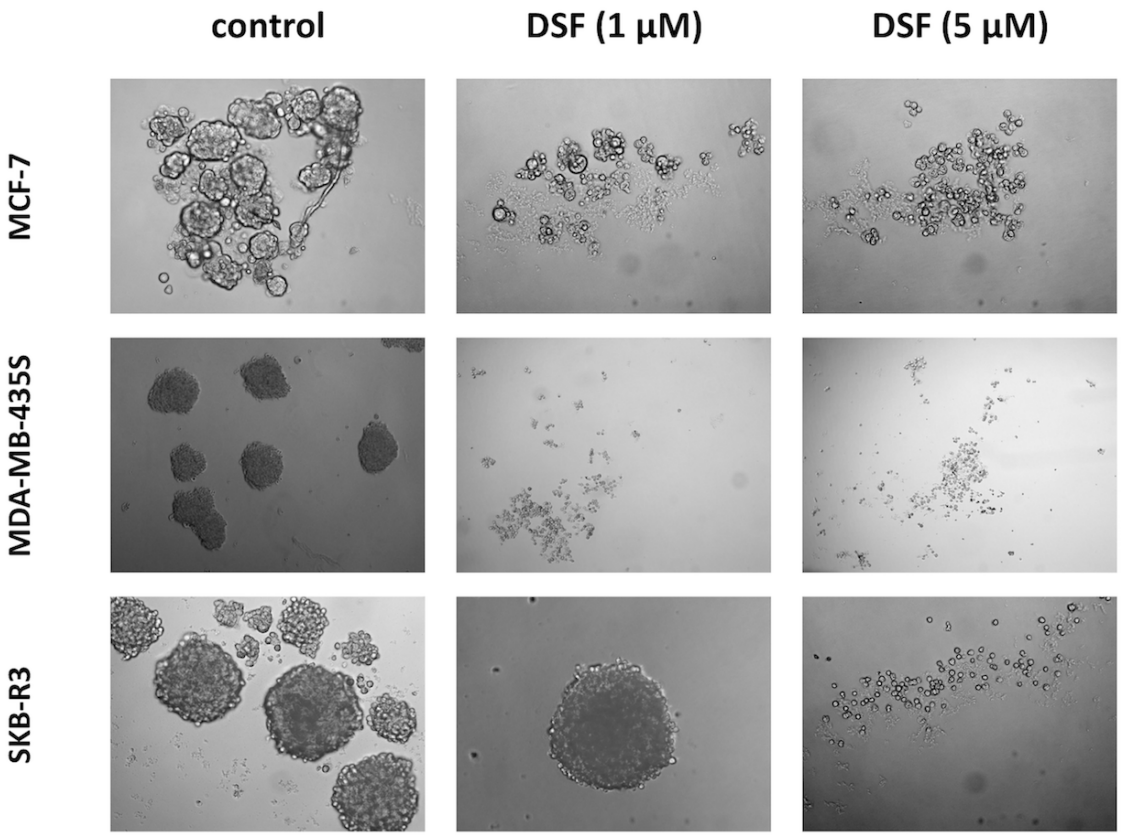


B

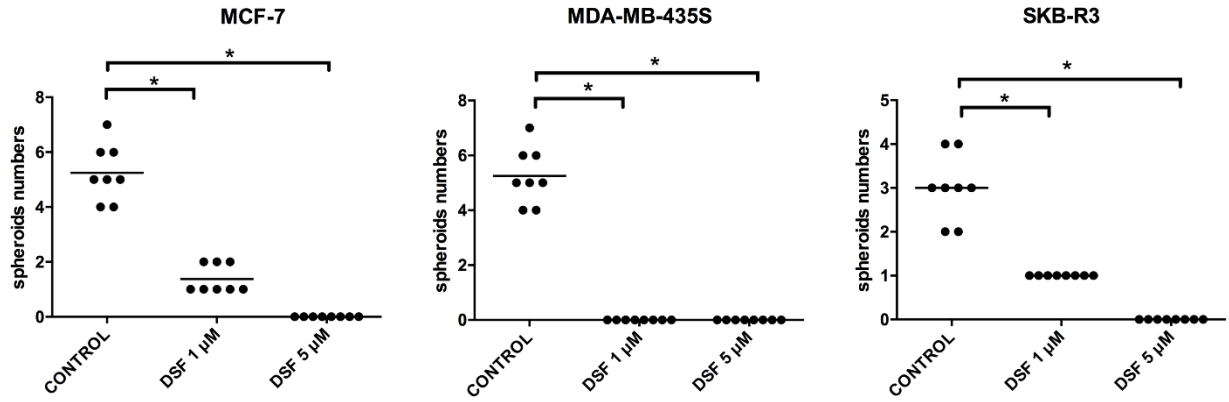


**Figure 2: Spheroid formation assay on breast cancer cell lines.**
A) Cells were cultured in 96-well ultra-low attachment plates without or with 1 µM or 5 µM DSF for 10 days and photographed (magnification 50 ×).
B) Cells were exposed to DSF for 10 days, and spheroids with ⩾ 100 µm in diameter were counted, and their numbers per well (n=8) were plotted. One representative of three independent experiments is shown.

## 5.3 Stemness-related markers are overexpressed in SDCs

We measured ALDH enzymatic activity of the SDCs of the three breast cancer cell lines and their parental MDCs to investigate the presence of a stem cell-like population using the ALDEFLUOR assay. As is shown in Figure 3, all SDCs had an increased proportion of ALDH-positive cells as compared to parental MDCs by FACS analysis. The proportion in this representative experiment increased from 10.8% to 46.1% in MCF-7, from 12.4% to 36.1% in MDA-MB-435S, from 27.1% to 31.3% in SKB-R3 cell line, in MDC and SDC, respectively. Next, we investigated mRNA expression of nuclear transcription factors (TF) Sox2, Oct3/4, and Nanog by which CSCs also share the stemness characteristics of embryonic stem cells. The mRNA levels detected by RT-PCR of Sox2, Oct3/4, and Nanog were all found to increase in SDCs of all three cell lines from 2-fold to almost 7-fold as compared to MDCs (Fig. 4). The results indicated that spheroids could enrich cancer stem cells and non-adherent 3D sphere models are reasonable to be used for evaluating stem cell activities in these breast cancer cell lines.

## 5.4 DSF inhibits ALDH activity in breast cancer cell lines

To determine the effective targeting of DSF on stem cells, ALDH activity in both MDCs and SDCs exposed to DSF (10 μM) was analyzed by ALDEFLUOR assay. As shown in Figure 3, the proportion of ALDH positive cells was decreased in both MDCs and SDCs after exposure to DSF: from 10.8% to 0.04% in MDCs and from 46.1% to 0.472% in SDCs in the MCF-7 cell line; from 12.4% to 0 in MDCs and from 36.1% to 0.02% in SDCs in the MDA-MB-435S cell line; and from 27.1% to 0 in MDCs and from 31.3% to 1.21% in SDCs in the SKB-R3 cell line. Importantly, the inhibitory effect of DSF was even stronger than the one of DEAB in both MDCs and SDCs. These results proved that DSF could target cancer stem cell characteristics in the investigated cell lines by inhibiting ALDH enzymatic activity.

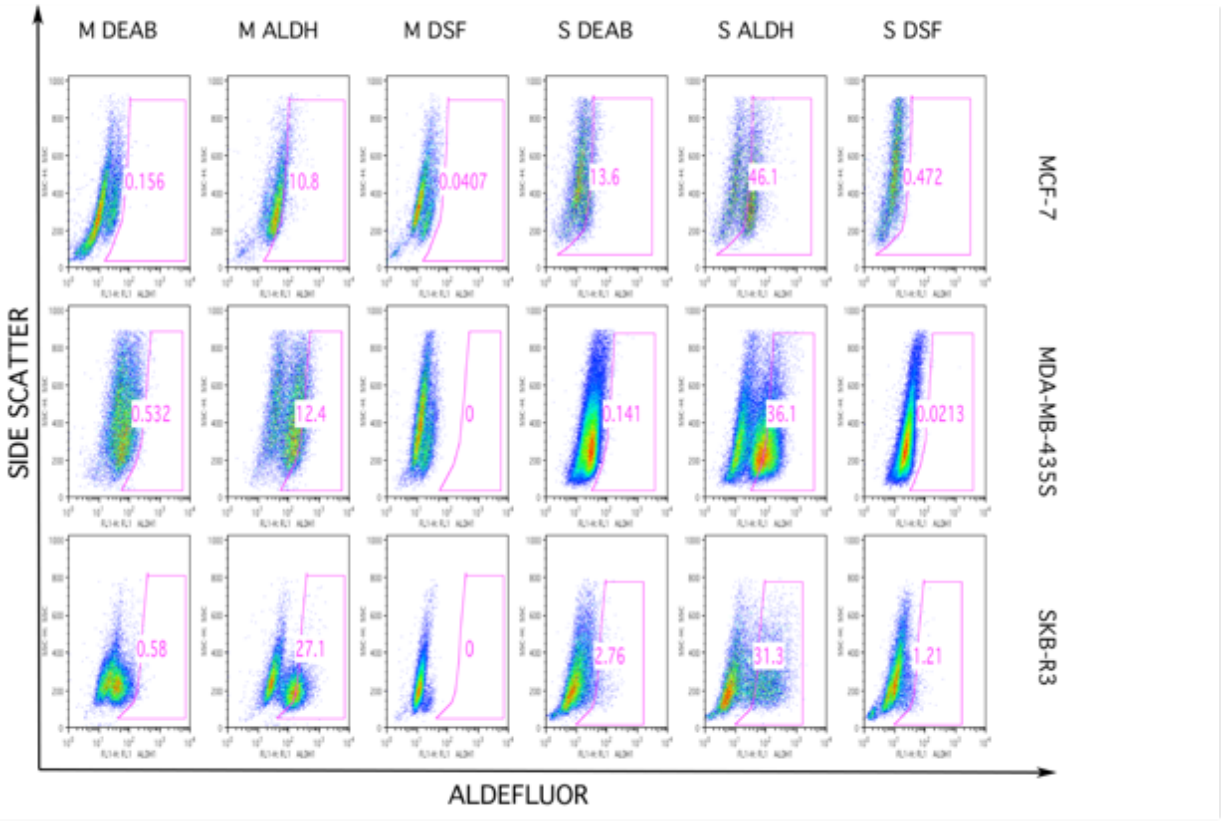


**Figure 3: Flow cytometric analysis of ALDH activity in breast cancer cell lines.**
MDC (M) and SDC (S) were exposed to DSF (10 μM), or control medium (ALDH) and ALDH activity was detected by ALDEFLUOR assay. Cells treated with diethylaminobenzaldehyde (DEAB), which is a specific ALDH inhibitor, were used as controls to establish the baseline fluorescence and define the cut-off for ALDEFLUOR-positive cells. One representative of three experiments is shown.

## 5.5 DSF inhibits stemness properties of SDCs

As we have shown that SDCs express higher levels of stemness-related nuclear transcription factors (TF) Sox2, Oct3/4, and Nanog in all three breast cancer cell lines, we further investigated the inhibitory effect of DSF on the stemness of SDCs by testing the expression of these CSC markers by qRT-PCR. As is shown in Figure 4, after DSF (1 μM) exposure for 48 h, mRNA levels of Sox2, Oct3/4, and Nanog in SDCs were all significantly decreased, and even lower than those observed in MDCs. This reduction was not accompanied by an obviously strong cytotoxic effect at this concentration, arguing against CSC depletion in cell lines MDA-MB-435S and SKB-R3, while in MCF-7, some cytotoxicity was noted. Further, the expression of these markers recovered swiftly when the cells were recultured in DSF-free medium for a further 48 h.

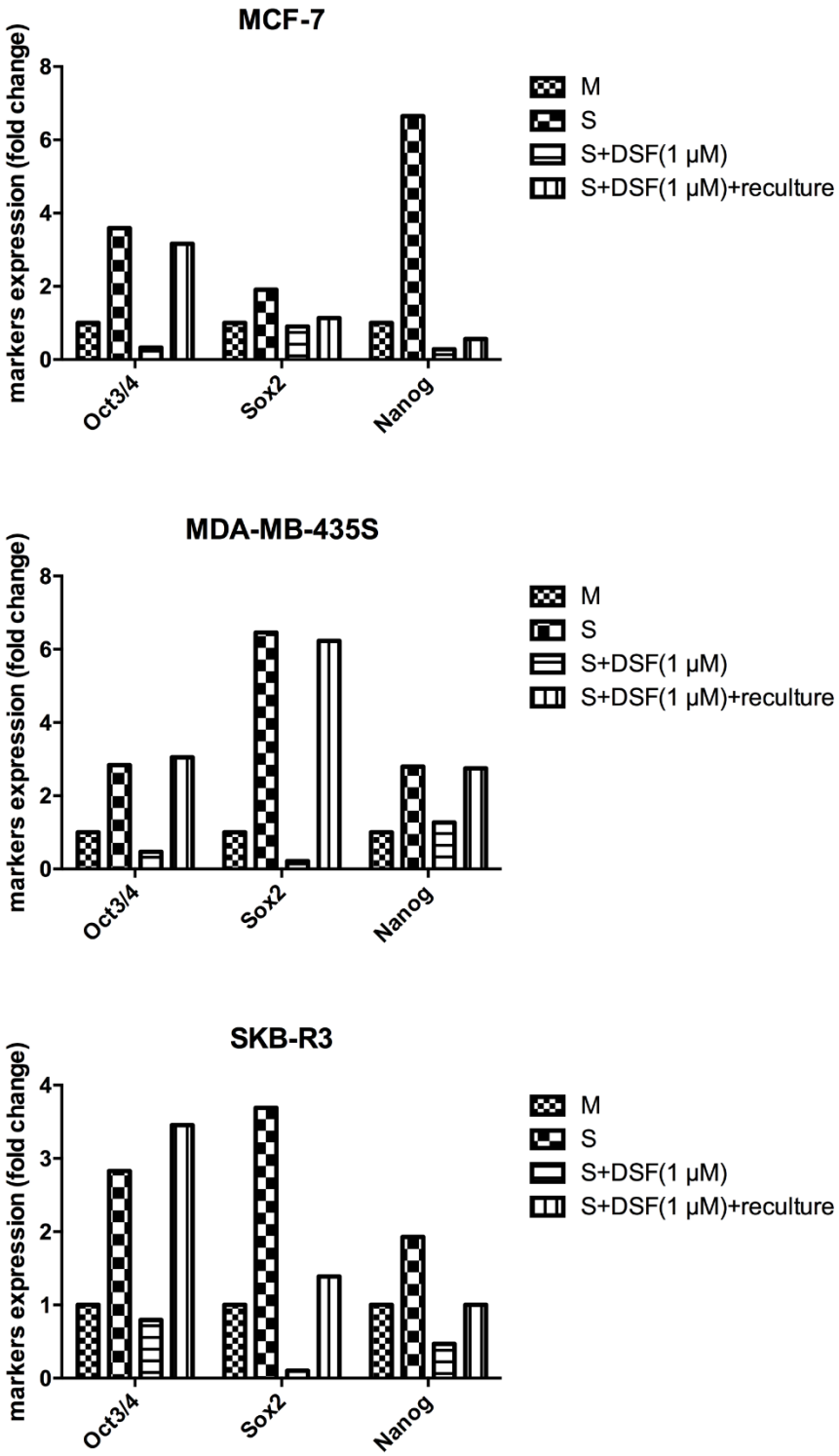


**Figure 4: Quantitative RT-PCR analysis of mRNA expression of stemness-related transcription factors.** The expression of stemness-related TF in MDC, SDC, DSF (1 μM, 48 h)-treated SDC, and SDC treated by DSF (1 μM, 48 h, followed by a phase to reculture in DSF-free medium for a further 48 h) was detected by qRT-PCR. M: MDC; S: SDC. One representative of three experiments is shown.

## 5.6 The combination of treatment with cisplatin and DSF induces more apoptosis

As DSF inhibited the stemness of CSCs, we wanted to further explore if DSF as an adjuvant treatment could be combined with a conventional chemotherapeutic agent like cisplatin, which rather targets the non-stemness cancer cells, to induce more apoptosis. Cells were exposed to DSF (1 µM) alone, cisplatin (5 µM) alone, or DSF (1 µM) plus cisplatin (5 µM) for 48 h, and the apoptotic status was evaluated using Annexin-V/PI staining by FACS analysis. The results revealed that generally more apoptosis was induced when cells were exposed to the combination treatment than either single drug alone. Both necrotic and apoptotic cell death was enhanced by both DSF and cisplatin treatment alone. As shown in Figure 5, the early and late apoptosis and necrosis together increased from 45.9% by treatment with cisplatin alone to 61.6% by the cisplatin/DSF combination treatment in MCF-7 cells, from 19.1% to 42.3% in MDA-MB-435S cells, and from 18.3% to 25.2% in SKB-R3 cells, respectively. Our results revealed that the combination of treatment with cisplatin and DSF induced more cellular apoptosis.

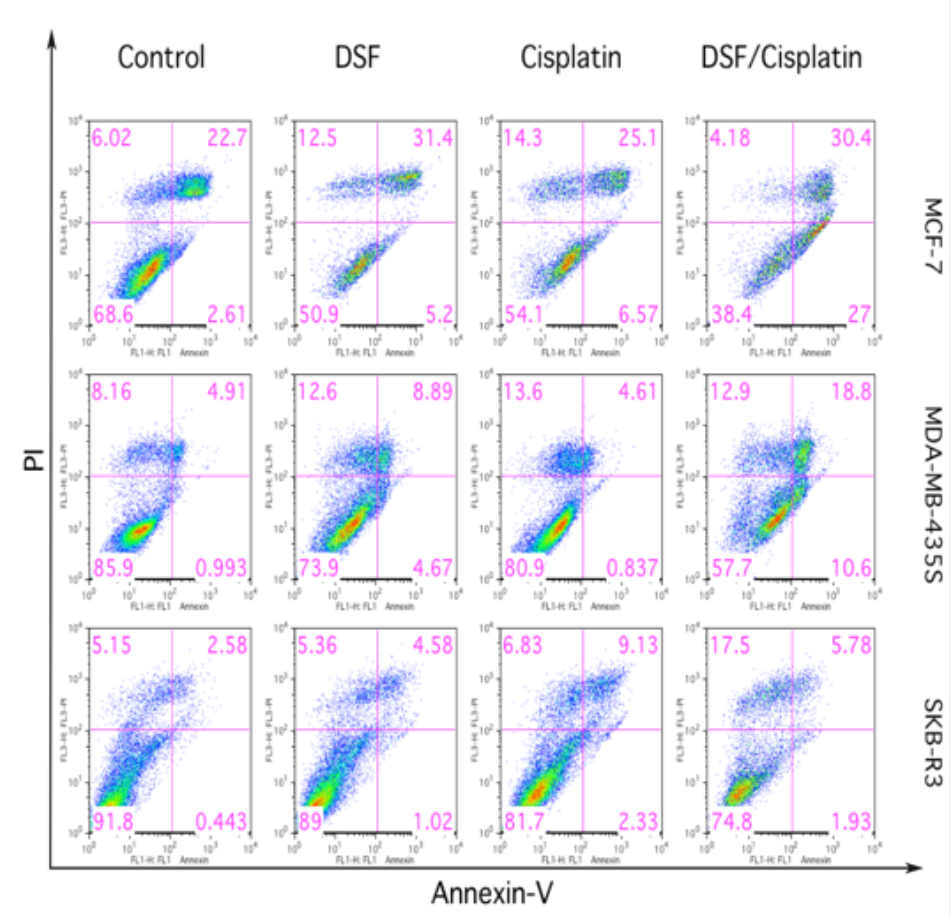


**Figure 5: Flow cytometric analysis of apoptosis assay.**
Cells were exposed to DSF (1 µM), Cisplatin (5 µM), or DSF (1 µM) plus Cisplatin (5 µM) for 48 h and the percentage of apoptotic cells was determined by Annexin-V/PI dual staining by

flow cytometric analysis.The Percentage of cells was determined in the four quadrants: live cells, (Annexin-V−/PI-, lower/left quadrant); early apoptotic cells (Annexin-V+/PI−, lower/right quadrant); late apoptotic cells (Annexin-V+/PI+, upper/right quadrant); and necrotic cells (Annexin-V−/PI+, upper/left quadrant), respectively. One representative of three experiments is shown.

## 5.7 DSF sensitizes breast cancer cells for cisplatin treatment

To determine whether DSF sensitizes for cisplatin treatment, all cells were treated with cisplatin alone or with cisplatin combined with DSF at a relatively low concentration (MCF-7: 0.3 μM; MDA-MB-435S and SKB-R3: 2 μM). We chose DSF at this concentration to avoid the cytotoxic effects exerted by DSF alone. An MTT assay was performed after 72 h exposure to the drugs. As shown in Figure 6, cisplatin/DSF combination treatment significantly reduced cell viability compared with cisplatin-treated cells ($P<0.05$). Cell viability dropped by 50% in MCF-7 cell line, 20%-30% in MDA-MB-435S cell line and SKB-R3 cell lines. These results indicate that DSF sensitizes breast cancer cells to cisplatin treatment even at a concentration where DSF is not toxic by itself.

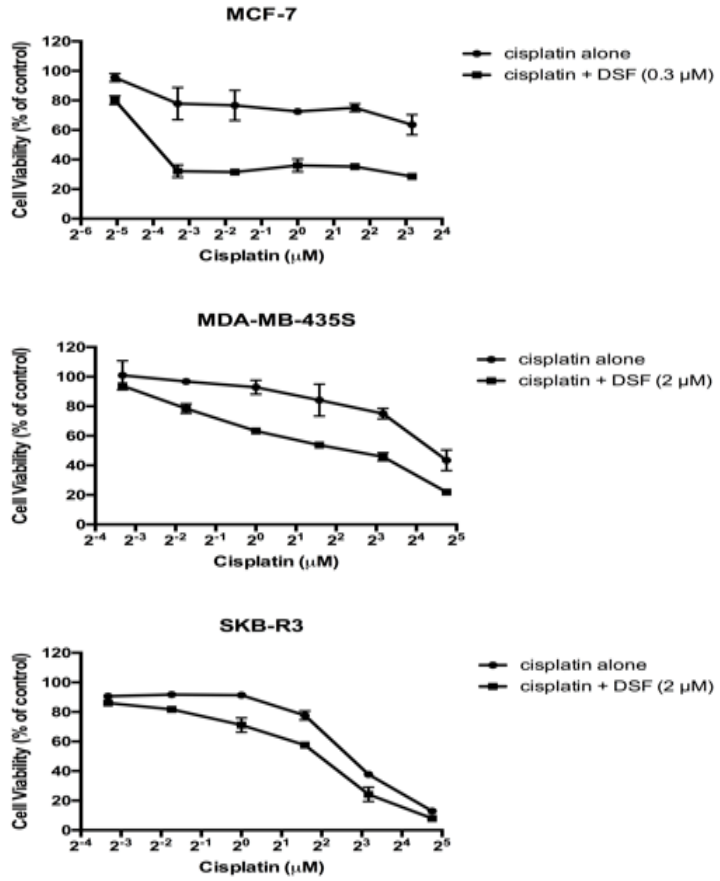


**Figure 6: DSF sensitizes breast cancer cells for cisplatin treatment.** MCF-7, MDA-MB-435S and SKB-R3 cells were treated with cisplatin alone or with cisplatin/DSF (2 μM) combination at

indicated concentrations for 72 h, followed by MTT assay for cellular viability. All data presented are representative of three independent experiments.

## 5.8 DSF overcomes cisplatin resistance in ALDH+ cells

Since DSF is an irreversible inhibitor of ALDH [59], and stem-like ALDH+ cells may play a role in cisplatin resistance [60], we next studied whether DSF combined with cisplatin could overcome cisplatin resistance. MCF-7 cells were flow-sorted with the ALDEFLUOR kit to isolate ALDH+ and ALDH- populations. ALDH+ and ALDH- cells were treated with different concentrations of cisplatin with/without DSF for 72 h, and were then subjected to an MTT assay. As shown in Figure 7, there was a significant difference in cellular viability between ALDH+ cells and ALDH- cells when they were treated with cisplatin alone. ALDH+ cells were more resistant to cisplatin treatment compared with ALDH- cells. However, when a low concentration of DSF (0.3 μM) was added, cellular viability decreased significantly (approx. 40%-50%) compared with cells treated with cisplatin alone, and there was no difference between ALDH+ cells and ALDH- cells, indicating that both ALDH+ cells and ALDH- cells were equally sensitive to DSF/cisplatin combination treatment. These results confirmed the potential efficacy of DSF in overcoming the cisplatin resistance on ALDH+ cells in this experimental setting.

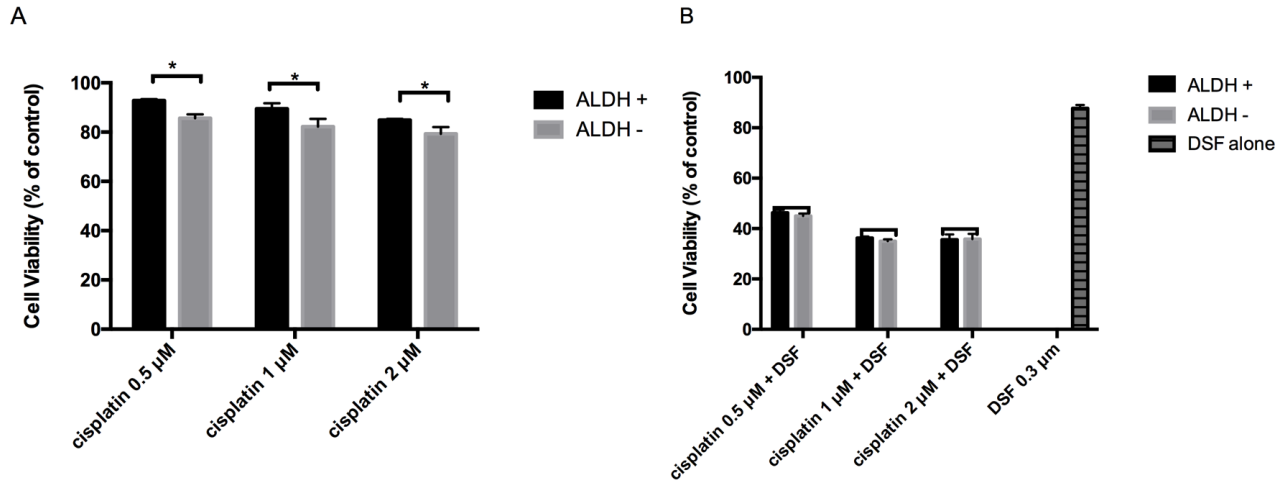


**Figure 7: DSF overcomes cisplatin resistance of ALDH+ cells.** ALDH+/- cells from MCF-7 were treated with (A) cisplatin alone, (B)cisplatin/DSF or DSF at indicated concentrations for 72 h. Cellular viability was determined by MTT assay. Cells without any drug treatment were used as controls. Each concentration was in triplicate. * $P < 0.05$.

## 5.9 DSF and cisplatin combined act synergistically

The combination index (CI) value was used as a quantitative measurement based on the mass-action law of the degree of drug interaction in terms of synergism and antagonism for a given endpoint of the effect measurement [42]. CI $<$ 0.1, CI 0.1-0.3, CI 0.3-0.7, CI 0.7-0.85, CI 0.85-0.9 and CI 0.90-1.10 indicate very strong synergism, strong synergism, synergism, moderate synergism, slight synergism, and nearly additive effects [42,43]. As shown in Table 1, the combination of DSF and cisplatin yielded a synergistic effect in all three tested cell lines at a broad concentration range from $IC_{50}$ to $IC_{90}$. Especially in MCF-7 cells, the CI value was 0.16 at the $IC_{90}$ level, and even less than 0.1 at $IC_{50}$ and $IC_{75}$ levels, indicating that a strong or very strong synergism was present. Synergism and moderate synergism were shown on MDA-MB-435S and SKB-R3 cells, respectively. And the dosage of each drug was reduced by 2-fold to several hundred-fold when compared with the dosage of each drug alone while maintaining the equal cytotoxic effect in combinations due to their synergistic effect.

**Table 1: Computer-simulated CI and DRI values for drug combinations at different levels of inhibition**

| Cis + DSF Combination | Combination Index at | | | Dose-Reduction Index at | | |
|---|---|---|---|---|---|---|
| | IC50 | IC75 | IC90 | IC50 | IC75 | IC90 |
| MCF-7 | 0.0023 | 0.014 | 0.16 | 454.89[a]<br>13586.7[b] | 84.67<br>382.40 | 15.76<br>10.76 |
| MDA-MB-435S | 0.35 | 0.36 | 0.38 | 2.96<br>66.36 | 2.81<br>115.65 | 2.67<br>201.56 |
| SKB-R3 | 0.64 | 0.75 | 0.88 | 2.34<br>4.78 | 1.85<br>4.82 | 1.47<br>4.87 |

[a]) fold reduction compared to single dose cisplatin
[b]) fold reduction compared to single dose DSF

## 5.10 Cisplatin arrests the cell cycle in G2 phase while DSF has no effect on cell cycle distribution

To explore the potent mechanism of DSF, cisplatin, and the combination, the distribution of cells in different phases of the cell cycle was evaluated after drug treatment. Cells were treated with DSF (1 μM), or cisplatin (1 μM, 5 μM) or the cisplatin/DSF combination for 72 h and cells cycle

distribution was analyzed by flow cytometry. As shown in Figure 8, in the MCF-7 cell line, a large sub-G1 peak appeared, indicating much apoptosis was induced because of the very strong synergistic effect. Therefore, an analysis of the cell cycle was not possible in this case, as the cell cycle phases disappeared and could no longer be identified. Thus, cell cycle distribution here was analyzed on SKB-R3 and MDA-MB-435S cell lines. MAD-MB-435S cells treated with 1 μM DSF showed no striking changes in cell cycle distribution (G1/S/G2 phase: 1 μM DSF vs. control= 49.9%/ 13.7%/ 23% vs. 54.8%/ 11.5%/ 20.7%). However, cells treated with 1 μM cisplatin had the cell cycle arrested in G2 phase as compared to the non-drug treated control cells (G2 phase: 1 μM cisplatin vs. control = 42.4% vs. 20.7%). Higher concentration of cisplatin at 5 μM induced stronger cell cycle arrest in the G2 phase (5 μM cisplatin vs. control = 45.4% vs. 20.7%) when compared to 1 μM cisplatin treatment. Similar results were also observed in the SKB-R3 cell line. These data suggested that cisplatin induced a cell cycle arrest in G2 phases which may further retard or prevent cell proliferation, while DSF had no effect on cell cycle distribution.

## 5.11 Cell cycle arrest in the DSF/cisplatin combination is due to cisplatin

To investigate the mechanism of the toxicity induced by the DSF/cisplatin combination, cell cycle distribution was assessed. As shown in Figure 8, SKB-R3 cells treated with DSF (1 μM)/cisplatin (1 μM) displayed a significant cell cycle arrest in G2 phases as compared to control cells (combination vs. control = 39.4% vs. 21.2%). The cell cycle distribution in the DSF (1 μM)/cisplatin (1 μM) combination was similar with cisplatin (1 μM) treatment alone (combination vs. cisplatin alone = G1: 35.8% vs. 42.9%; S: 16.1% vs. 15.5%; G2: 39.4% vs 30.9%). Also, cells treated with DSF (1 μM)/cisplatin (5 μM) exhibited a significant cell cycle arrest in G2 phases, and cell cycle distribution in the DSF (1 μM)/cisplatin (5 μM) combination was similar to 5 μM cisplatin treatment alone (combination vs. cisplatin alone = G1: 8.95% vs. 5.79%; S: 36% vs. 32.1%; G2: 38.7% vs 54%). Similar results were observed on MDA-MB-435S cell line. These results indicated that cell cycle changes in the combination treatment were due to the effect of cisplatin.

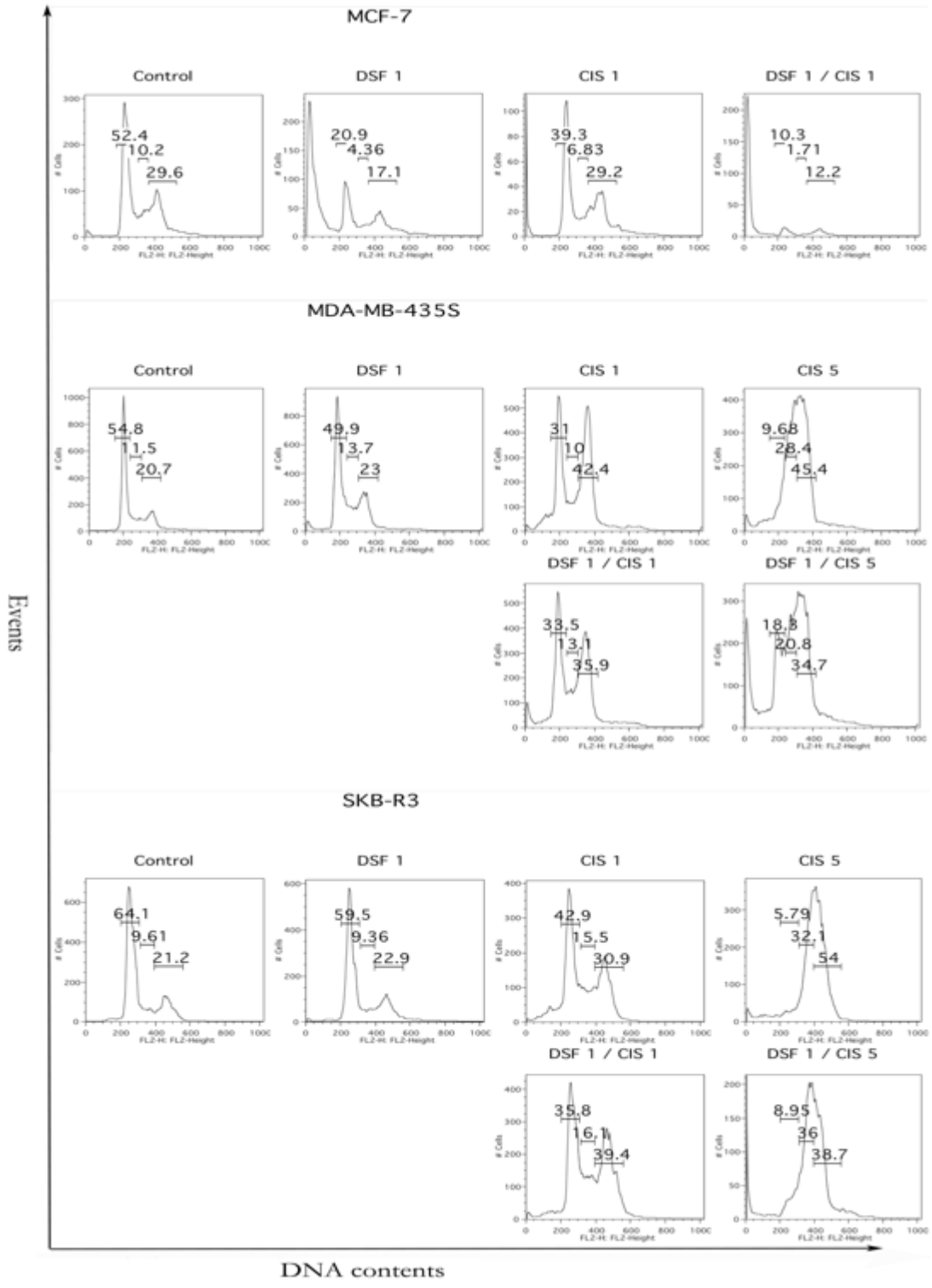


**Figure 8: Cell cycle analysis by FACS.** Cells were treated with DSF (1 μM), or cisplatin (1 μM, 5 μM), or cisplatin/DSF combination for 72 h, DNA content distribution was analyzed using flow cytometry. Gated numbers marked in figures are the percentage of G0/G1, S, G2/M phases. CIS: Cisplatin; DSF: Disulfiram.

## 5.12 ROS accumulation by DSF is concentration-dependent and time-dependent

ROS are involved in cancer development and metastasis. We have shown that DSF inhibits ALDH activity which normally acts as a ROS scavenger to protect cells against oxidative stress. Thus, it is important to further investigate if the underlying mechanisms of DSF toxicity are based on ROS production.

Firstly, we examined different concentrations of DSF and a DSF/cisplatin combination with short time treatment. All cells were treated with DSF (10 μM, 100 μM), or cisplatin (10 μM, 100 μM) or the cisplatin/DSF combinations for 4 h, intracellular ROS activity was analyzed by flow cytometry. As shown in Figure 9, there was no ROS generated when the cells were treated with 10 μM DSF for 4 h compared with no drug treated control cells in all three cell lines. ROS was generated in all three cell lines when the concentration of DSF increased to 100 μM. Interestingly, no ROS was generated by cisplatin during the 4 h treatment period. These data indicated that ROS was quickly generated by DSF at high concentrations, which may cause an instant and short-term cytotoxicity to cancer cells.

Since it's hard to generate ROS by DSF treatment at low concentration in a short time frame, we next performed the time course experiment with relatively low concentration of DSF at 10 μM. All three breast cancer cells were treated with DSF (10 μM), cisplatin (10 μM), or the DSF (10 μM)/cisplatin (10 μM) combination for 10 h, 20 h, and 56 h, respectively. As shown in Figure 10, after 10 h exposure, there was no ROS generation in either DSF treated-cells, cisplatin treated-cells, not even in the DSF/cisplatin combination treated-cells in MCF-7 and SKB-R3 cell lines. Detectable ROS was generated only in DSF/cisplatin combination in the MDA-MB-435S cell line. After 20 h exposure, ROS was generated in DSF treated-cells in MCF-7 and SKB-R3 cell lines, as well as in DSF/cisplatin combination-treated cells in three cell lines. However, when the cells were treated with the indicated drugs for 56 h, apparently an increasing amount of ROS was generated in DSF-treated cells and cisplatin-treated cells as well as DSF/cisplatin combination treated-cells in all three cell lines. These results indicated that ROS accumulated by DSF at low concentration is time-dependent.

## 5.13 DSF/cisplatin enhances the generation of ROS as compared to single drug treatment

Since ROS is generated by DSF treatment at high concentration in a short time frame, or at low concentrations over a longer time period, we were next interested in the ROS generation by the DSF/cisplatin combination and the contribution of each drug in the combination for ROS generation. As shown in Figures 9 and 10, cells exposed to DSF/cisplatin generated more ROS than by each single drug treatment, no matter whether the treatment was short- or long- time treatment. Interestingly, as shown in the last column in Figure 9, when cells were treated with high concentrations of DSF (100 μM)/cisplatin (100 μM) for 4 h, the ROS generation curve in the drug combination is quite similar to DSF alone, indicating that ROS generation in short-term treatment in the combination is mainly due to high concentrations of DSF. However, both DSF and cisplatin contributed to the total ROS generation in combinations when cells were exposed to drugs for 56 h (Figure 10).

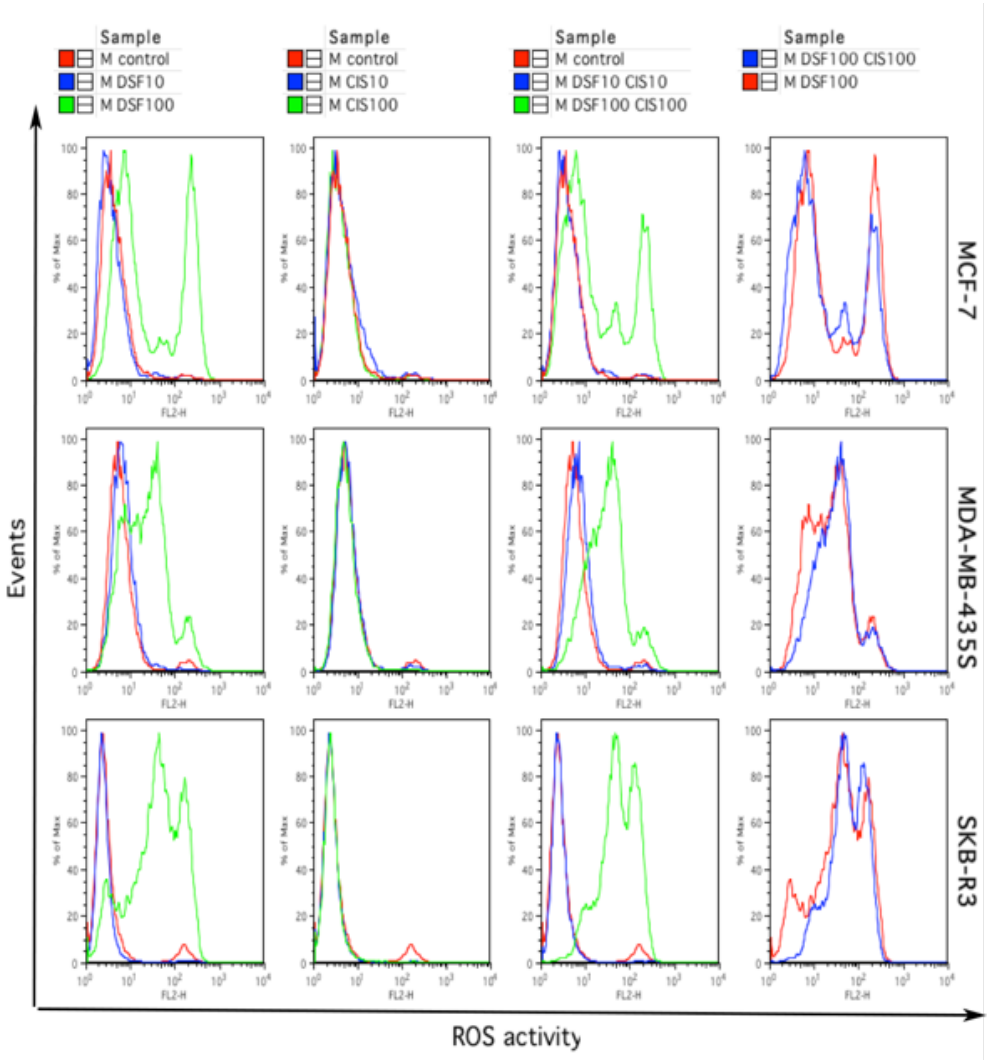


**Figure 9: ROS production during short term in drug-treated cells**. Cells were exposed to DSF (10 μM,100 μM), or cisplatin (10 μM,100 μM), or combinations for 4 h before they were harvested for ROS measurement by flow cytometry. CIS: Cisplatin. M: monolayer-derived cells.

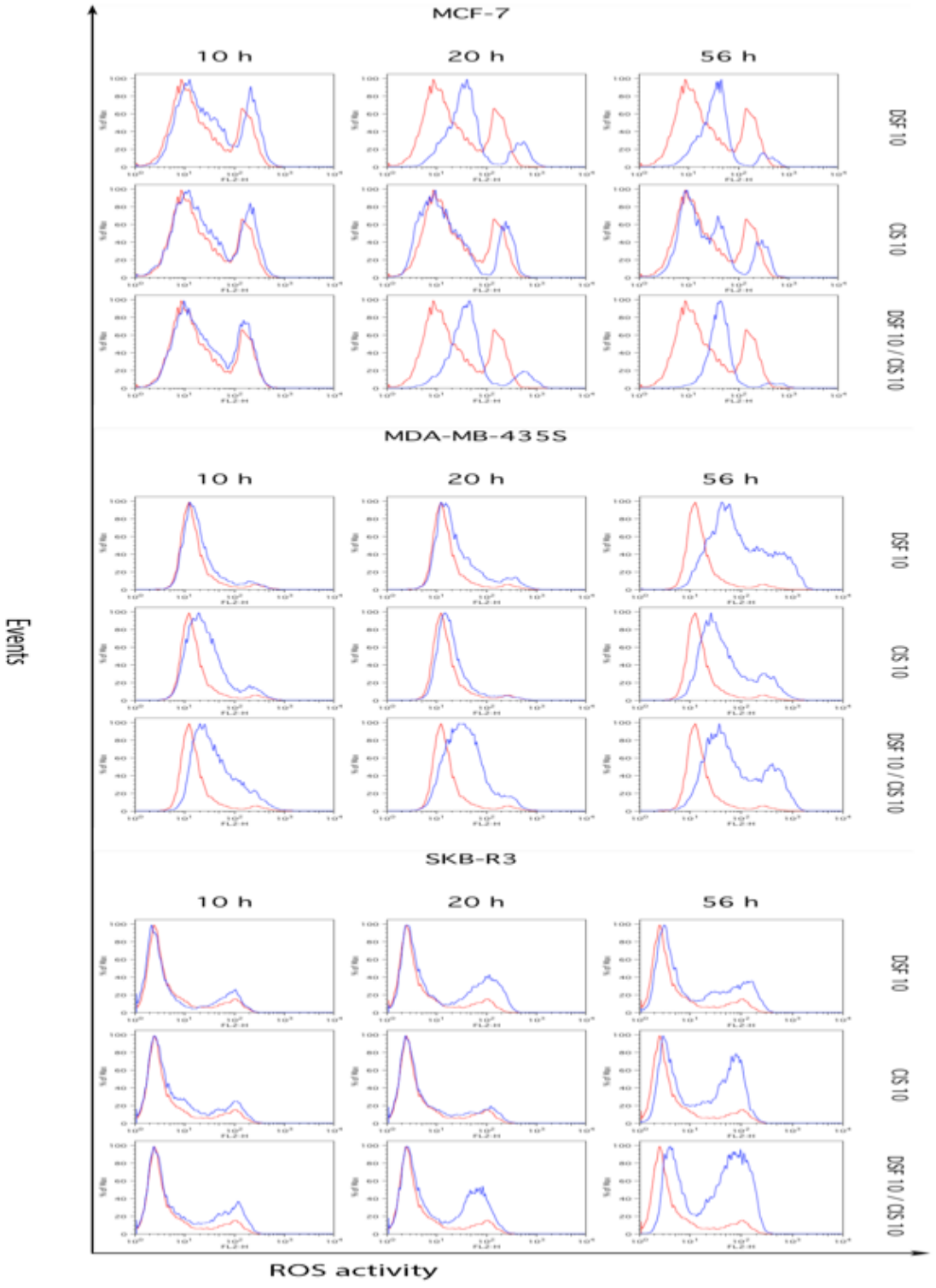


**Figure 10: Time course of ROS production by FACS.** Cells were exposed to DFS, or cisplatin or combinations for 10 h, 20 h, and 56 h. Red lines represent the untreated control cells and blue lines represent drug-treated cells. CIS: Cisplatin; DSF: Disulfiram.

## 5.14 Cell cycle and ROS generation in ALDH+/- cells

To further explore whether DSF has different effects on ALDH+ and ALDH- cells, both ALDH+ cells and ALDH- cells were treated with DSF (0.3 μM) and cisplatin (2 μM), respectively. The effect of cisplatin on cell cycle change and the effect of DSF on ROS generation was observed. As shown in Figure 11A, ALDH- cells were more sensitive to cisplatin treatment, with G0/G1 decreasing from 58.3% to 39.5% and G2 increasing from 25.7% to 42.6%. ALDH+ cells were more resistant to cisplatin treatment, with G0/G1 decreasing only from 65.1% to 55.4% and G2 increasing from 24.3% to 30%. As shown in Figure11B, ALDH- cells contain higher levels of ROS due to rapid metabolism, while ALDH+ cells are more quiescent with lower levels of ROS. ROS generation was increased in both ALDH+ and ALDH- cells when they were treated with DSF compared to non-drug-treated control cells. ROS production by ALDH+ cells and ALDH- cells reached the same level after DSF treatment. Concerning the relative increase, ALDH+ cells showed a greater increase than ALDH- cells, as they contain lower basic levels of ROS.

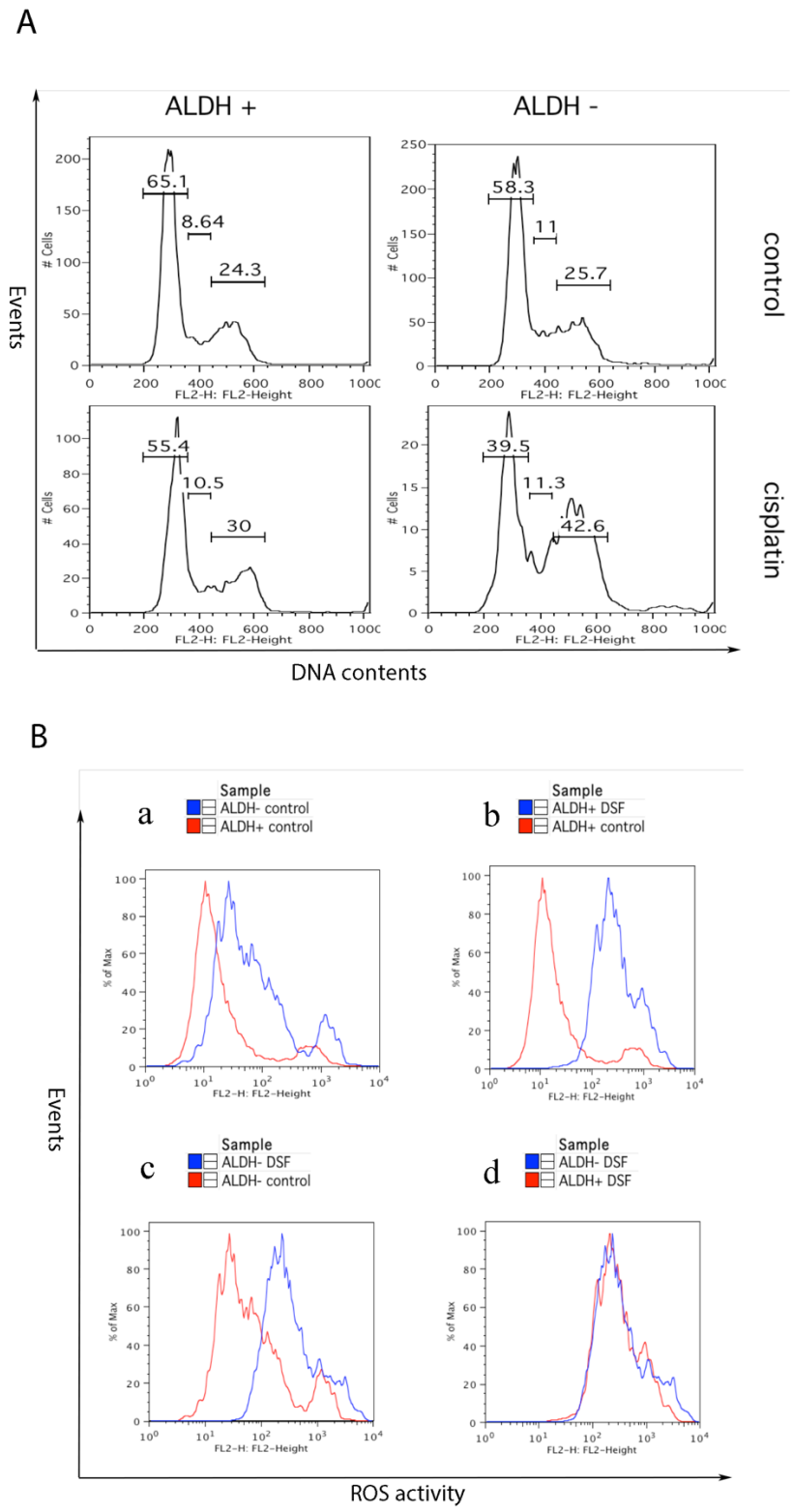


**Figure 11: Cell cycle analysis and ROS production of ALDH+ and ALDH- cells by FACS.** A) The effect of cisplatin (2 µM, 72 h) on cell cycle change on ALDH+/- cells. B) The effect of DSF (0.3 µM, 72 h) on ROS production on ALDH+/- cells. a) ALDH+/- control; b) ALDH+ DSF/control; c) ALDH- DSF/control; d) ALDH+/- DSF.

# 6 Discussion

Breast cancer is the second leading cause of cancer death in women worldwide [1]. Despite the impressive clinical improvements of breast cancer therapies, mortality for breast cancer patients is mostly related to late diagnosis and resistance to systemic therapy, leading to metastasis and recurrence. One of the main obstacles that hinder therapeutic success in breast cancer is the presence of subpopulations of cancer stem cells (CSCs) that are undifferentiated and self-renewing, and that are held responsible for tumorigenicity and drug resistance [61,62]. Because a majority of anti-cancer drugs target actively dividing cells, quiescent CSCs remain relatively unaffected and may be the cause for relapse, progression, and dissemination of cancer. Therefore, a more efficient anti-cancer therapy is expected to be targeting also CSCs.

Different approaches have been used to identify and isolate CSCs. We decided to enrich for CSCs by spheroid culture models. Spheroids are three-dimensional clusters of cultured tumor cells which simulate the tumor in vivo better than adherently growing cells [63]. A wealth of experiments have shown that SDC exhibit stem cell properties and display the phenotype of CSCs in different tumor types [64-66]. Here, we also provided evidence that SDC showed a higher proportion of ALDH positivity in all three breast cancer cell lines investigated. In addition to ALDH, the expression of stemness-related transcription factors Oct3/4, Sox2, and Nanog was also 2-fold to 7-fold higher in SDC as compared to MDC. Our results are in agreement with results from other labs which also report that there is an enrichment of CSCs according to ALDH and stemness-related transcription factor expression by anchorage-independent culture techniques and thus spheroid cell culture models could be used for evaluating characteristics of CSCs [67, 68].

In this study, we firstly confirmed that DSF itself exhibits dose-dependent cytotoxicity in the three breast cancer cell lines investigated. We also demonstrated that the ALDH level was significantly higher in SDCs than in MDCs. The ALDH activity was significantly inhibited by DSF in SDCs, supporting a role for DSF in treatment of the ALDH positive subpopulation. Importantly, a suppressive effect of DSF on the stemness of ALDH+ CSC, as shown by inhibition in a sphere formation assay. In addition, several stemness-related nuclear transcription factors associated with breast CSCs including Oct3/4, Sox2, and Nanog were also higher expressed in SDCs than MDCs. Our results are in agreement with previous reports that the expression of stemness transcription factors Sox2, Oct3/4, and Nanog, was increased in CSCs

and contributes to plasticity, self- renewal, and stemness [69]. Notably, DSF at 1 μM markedly suppressed the mRNA level of Oct3/4, Sox2, and Nanog in SDC. Their mRNA expression levels were even lower in SDCs than in MDCs after DSF exposure. We speculate that the deceased expression of CSC markers could be due to two reasons: firstly, CSC were specifically killed, resulting in the reduction of stemness transcription factor positive cells in the population, or secondly stemness factor transcription by CSC was inhibited by DSF while the cells were still alive. In order to discriminate these options, we re-cultured the cells for two more days in drug-free fresh medium after DSF exposure. We found that the expression of CSC markers quickly recovered after this phase, and in most cases returned to the original level of SDCs. Since DSF is an irreversible inhibitor of ALDH [70], the results indicate that the stem cells were not killed in these conditions but the stemness characteristics of cells were rather inhibited. These results are consistent with our data from the spheroid formation assay. The number of spheroids were reduced remarkably when cells were exposed to 1 μM DSF, and the capacity to form spheroids was completely inhibited when cells were exposed to 5 μM DSF, indicating that both concentrations of 1 μM and 5 μM DSF inhibited the stemness of CSCs in the absence of overt cytotoxic effects.

Next, we explored the combination effect of DSF and cisplatin. Cisplatin is currently one of the most effective chemotherapeutic agents used for breast cancer treatment. Cisplatin unfolds its cytotoxicity by binding to nuclear DNA and thereby interferes with the normal DNA replication mechanisms [71]. However, there are two unsolved obstacles related to the utilization of cisplatin: resistance and toxicity [72]. Resistance or insensitivity of tumor cells to cisplatin treatment is an essential reason for relapse. The combination of cisplatin with other chemotherapeutic drugs has obtained satisfactory clinical results, but also caused greater toxicity for patients.

This study demonstrated that the combination treatment of cisplatin and DSF induced more cellular apoptosis than each individual treatment. What's more, the results showed that DSF sensitizes breast cancer cell lines to cisplatin treatment. This obvious chemo-sensitizing effect of DSF was observed in this study even at its low concentration that does not display any cytotoxicity on its own. Our results have also shown that ALDH+ cells were more resistant to cisplatin treatment than ALDH- cells. This is in agreement with studies from other labs which demonstrated that cancer cells expressing stem cell markers are highly resistant to radio- and chemotherapy [73]. Based on these results, we examined the resistance-reversing effect of DSF

in this study. Our results showed that both ALDH+ cells and ALDH- cells exhibited equal sensitivity to DSF/cisplatin combination treatment, indicating that DSF overcomes cisplatin resistance of ALDH+ cells. One explanation could be that ALDH activity of ALDH+ cells is inhibited by DSF, leaving ALDH+ cells and ALDH- cells equally sensitive to DSF and cisplatin treatment.

Next, we used a quantitative method to determine the combination effect of DSF and cisplatin. The results showed that DSF and cisplatin yielded a synergistic effect at broad effect levels ranging from $IC_{50}$ to $IC_{90}$ in all three breast cancer cell lines. The highest degree of synergism was observed in the MCF-7 cell line. The CI value was 0.16 at $IC_{90}$ level, and even less than 0.1 at $IC_{50}$ and $IC_{75}$ levels, indicating a strong or very strong synergism. Due to this synergistic effect, the dosage of each drug may be reduced by 2-fold or even hundred-fold while maintaining the equal cytotoxicity when they are combined. This synergistic effect in a DSF/cisplatin combination may provide many therapeutic benefits in clinical treatment regimens against breast cancers. The most important consequence is that it could increase or at least maintain the same efficacy but decrease the dosage of each drug to reduce toxicity, thereby potentially reducing the toxicity toward normal tissues.

To explore the possible mechanism of DSF and cisplatin in combination treatment, cell cycle analysis and ROS generation was determined in this study. Studies have shown that cisplatin induces cross-linking of DNA [71], therefore inducing a G2/M arrest. Our results also showed that cisplatin arrested cell cycle distribution in the G2 phase. However, DSF had no significant effect on cell cycle distribution. In DSF/cisplatin combination treated cells, cell cycle distribution was very similar to that in cisplatin single treatment, indicating that cell cycle arrest in DSF/cisplatin combination was mainly due to the cisplatin effect.

As we have shown that DSF inhibits ALDH activity which normally acts as a ROS scavenger to protect cells against oxidative stress, we further explored the relationship between ROS generation and DSF concentration and exposure time. The results showed that DSF induced ROS accumulation in a dose-dependent manner. Higher concentration of DSF could induce more ROS accumulation in cells. Interestingly, high concentration of DSF could also induce ROS accumulation in a very short time, indicating that DSF can cause instant killing of cells [74]. In the DSF/cisplatin combination treatment at high concentration in a short time period, DSF was responsible for most of the ROS accumulation. Low concentration of DSF needed longer time to

induce cells to accumulate ROS, and both DSF and cisplatin contributed to the ROS accumulation at lower concentration drug combinations.

The effect of cisplatin on cell cycle distribution and the effect of DSF on ROS accumulation was further determined after cell sorting. The results indicated that ALDH+ cells showed cancer stem-like properties, with low levels of ROS, while ALDH- cells were more proliferating with higher levels of ROS due to rapid metabolism. Upon treatment. more ROS accumulated in ALDH+ cell, reaching the same levels of ROS in ALDH- cells, finally. These results indicated that DSF showed, at least, equal cytotoxic  it to ALDH+/- cells. However, concerning the relative increase, ALDH+ cells showed a greater increase than ALDH- cells, as they contain lower basic levels of ROS, indicating that ALDH+ cells might be more sensitive to DSF treatment.

In considerin ins  all results we obtained in this study, we summarize the possible mechanisms for the synergistic effect of DFS and cisplatin combination as follows: 1) DSF suppresses ALDH activity and stemness of CSCs, reverses cisplatin resistance on ALDH+ cells, and sensitizes cisplatin-resistant CSCs population to cisplatin treatment, consequently improving the ability of cisplatin to kill resistant or less sensitive cancer cells. This is in agreement with a study by Wantong Song et al. [75] that DSF improved the effectiveness of cisplatin in resistant lung cancer cell lines. 2) DSF and cisplatin exert their cytotoxicity based on different mechanisms. DSF induces cellular apoptosis by accumulation of ROS, including instant killing and delayed cytotoxicity, while cisplatin induces apoptosis based on the DNA damage, leading to the cell cycle distribution changes, and increased ROS generation during longer treatment periods. 3) Cisplatin and DSF exert their cytotoxicity on different targeted cell types. The conventional chemotherapy agent cisplatin targets proliferating cells with little effect on CSCs, while DSF is equally cytotoxic to both proliferating cells and ALDH+ “stem-like” cells and renders CSC more sensitive to cisplatin. One other scenario could be that DSF by inhibiting ALDH activity, renders ALDH+/- cells equally sensitive to cisplatin cytotoxicity. This is in agreement with results from other labs demonstrating that DSF targets ALDH-positive cells in breast cancer [76, 77].

Taken together, this study provides evidence that cells with CSC-like properties exists in SDC from breast cancer cell lines. These cells are characterized by increased ALDH activity and a higher level of stemnness-related transcription factor expression. We demonstrated that DSF

effectively inhibited ALDH positive cell populations and targeted CSC-ALDH to further inhibit the stemness of CSCs, and in turn, induced more cellular apoptosis by combination with the conventional anti-cancer agent cisplatin. Results from the present study demonstrated significant cisplatin-sensitizing effects of DSF on breast cancer cell lines, a cisplatin resistance-reversing effect, and a synergistic effect, described the possible mechanisms of the enhanced efficacy of the DSF/cisplatin combination. Because of the sensitizing and synergistic effects of the drug combination, DSF may be used as a novel adjuvant and be incorporated into conventional regimens to improve the effectivity of targeted chemotherapy for breast cancer treatment in future. However, more research is needed to further verify the inhibitory effects of DSF in animal experiments on xenotransplanted tumor models, and for clinical trials the safe application and effective dose of DSF in patients, as well as the pharmacologic limitations such as first-pass-effects have to be further defined.

# 7 References


1. R. Siegel, D. Naishadham, A. Jemal. Cancer Statistics. CA Cancer J. Clin, 2013; 63: 11-30.

2. Ferzoco R.M., Ruddy K.J. The epidemiology of male breast cancer. Curr Oncol Rep, 2016; 18:1.

3. Lukong KE. Understanding breast cancer-The long and winding road. BBA Clin, 2017; 7: 64-77.

4. Leong SP, Shen ZZ, Liu TJ, Agarwal G, Tajima T, Paik NS, Sandelin K, Derossis A, Cody H, Foulkes WD. Is breast cancer the same disease in Asian and Western countries? World J Surg, 2010; 34: 2308-2324.

5. Collaborative Group on Hormonal Factors in Breast Cancer. Menarche, menopause, and breast cancer risk: individual participant meta-analysis, including 118 964 women with breast cancer from 117 epidemiological studies. Lancet Oncol, 2012; 13: 1141-1151.

6. Yu Z, Guo X, Jiang Y, Teng L, Luo J, Wang P, Liang Y, Zhang H. Adjuvant endocrine monotherapy for postmenopausal early breast cancerpatients with hormone-receptor positive: a systemic review and network meta-analysis. Breast Cancer, 2018; 25: 8-16.

7. Tremont A, Lu J, Cole JT. Endocrine Therapy for Early Breast Cancer: Updated Review. Ochsner Journal, 2017; 17: 405-411.

8. Buzdar AU. Role of biologic therapy and chemotherapy in hormone receptor- and HER2-positive breast cancer. Ann Oncol, 2009; 20: 993-999.

9. Slamon DJ, Leyland-Jones B, Shak S, Fuchs H, Paton V, Bajamonde A, Fleming T, Eiermann W, Wolter J, Pegram M, Baselga J, Norton L. Use of chemotherapy plus a monoclonal antibody against HER2 for metastatic breast cancer that overexpresses HER2. N Engl J Med, 2001; 344: 783-792.

10. Anders CK, Carey LA. Biology, metastatic patterns, and treatment of patients with triple-negative breast cancer. Clin Breast Cancer, 2009; 9: S73–81.

11. Dodwell D, Williamson D. Beyond tamoxifen: extended and late extended endocrine therapy in postmenopausal early breast cancer. Cancer Treat Rev, 2008; 34: 137-144.

12. Ismail-Khan R, Bui MM. A review of triple-negative breast cancer. Cancer Control, 2010; 17: 173-176.

13. Goldhirsch A, Winer EP, Coates AS, Gelber RD, Piccart-Gebhart M, Thürlimann B, Senn HJ; Panel members. Personalizing the treatment of women with early breast cancer: highlights of the St Gallen International Expert Consensus on the Primary Therapy of Early Breast Cancer 2013. Ann Oncol, 2013; 24: 2206-2223.

14. Foulkes WD, Smith IE, Reis-Filho JS. Triple-negative breast cancer. N Engl J Med, 2010; 363: 1938-1948.

15. Yardley DA. Drug resistance and the role of combination chemotherapy in improving patient outcomes. Int J Breast Cancer, 2013; 2013: 137414.

16. Longley DB, Johnston PG. Molecular mechanisms of drug resistance. Journal of Pathology, 2005; 205: 275-292.

17. Gottesman MM, Fojo T, Bates SE. Multidrug resistance in cancer: role of ATP-dependent transporters. Nature Reviews Cancer, 2002; 2: 48-58.

18. Lapidot T, Sirard C, Vormoor J, Murdoch B, Hoang T, Caceres-Cortes J, Minden M, Paterson B, Caligiuri MA, Dick JE. A cell initiating human acute myeloid leukemia after transplantation in SCID mice. Nature, 1994; 367: 645-648.

19. Magee JA, Piskounova E, Morrison SJ. Cancer stem cells: impact, heterogeneity, and uncertainty. Cancer Cell, 2012; 21: 283-196.

20. Friedmann-Morvinski D and Verma IM. Dedifferentiation and reprogramming: origins of cancer stem cells. EMBO Rep, 2014; 15: 244-253.

21. Bao L, Cardiff RD, Steinbach P, Messer KS, Ellies LG. Multipotent luminal mammary cancer stem cells model tumor heterogeneity. Breast Cancer Res, 2015; 17: 137.

22. Liu S, Cong Y, Wang D, Sun Y, Deng L, Liu Y, Martin-Trevino R, Shang L, McDermott SP, Landis MD, Hong S, Adams A, D'Angelo R, Ginestier C, Charafe-Jauffret E, Clouthier SG, Birnbaum D, Wong ST, Zhan M, Chang JC, Wicha MS. Breast Cancer Stem Cells Transition between Epithelial and Mesenchymal States Reflective of their Normal Counterparts. Stem Cell Reports, 2013; 2: 78-91.

23. Sin WC, Lim CL. Breast cancer stem cells-from origins to targeted therapy. Stem Cell Investig, 2017; 4: 96.

24. Ma R, Bonnefond S, Morshed SA, Latif R, Davies TF. Stemness is Derived from Thyroid Cancer Cells. Front Endocrinol, 2014; 5: 114.

25. Al-Hajj M1, Wicha MS, Benito-Hernandez A, Morrison SJ, Clarke MF. Prospective identification of tumorigenic breast cancer cells. Proc Natl Acad Sci U S A, 2003; 100: 3983-3988.

26. Badve S, Nakshatri H. Breast-cancer stem cells-beyong semantics. Lancet Oncol, 2012; 13: e43-e48.

27. Yang F, Xu J, Tang L, Guan X. Breast cancer stem cell: the roles and therapeutic implications. Cell Mol Life Sci, 2017; 74: 951-966.

28. Fillmore CM, Kuperwasser C. Human breast cancer cell lines contain stem-like cells that self-renew, give rise to phenotypically diverse progeny and survive chemotherapy. Breast Cancer Res, 2008; 10: R25.

29. Ahmed MA1, Aleskandarany MA, Rakha EA, Moustafa RZ, Benhasouna A, Nolan C, Green AR, Ilyas M, Ellis IO. A $CD44^{-}/CD24^{+}$ phenotype is a poor prognostic marker in early invasive breast cancer. Breast Cancer Res Treat, 2012; 133: 979-995.

30. Ginestier C, Hur MH, Charafe-Jauffret E, Monville F, Dutcher J, Brown M, Jacquemier J, Viens P, Kleer CG, Liu S, Schott A, Hayes D, Birnbaum D, Wicha MS, Dontu G. ALDH1 is a marker of normal and malignant human mammary stem cells and a predictor of poor clinical outcome. Cell Stem Cell, 2007; 1: 555-567.

31. Charafe-Jauffret E, Ginestier C, Bertucci F, Cabaud O, Wicinski J, Finetti P, Josselin E, Adelaide J, Nguyen T-T, Monville F. ALDH1-positive cancer stem cells predict engraftment of primary breast tumors and are governed by a common stem cell program. Cancer Res, 2013; 73: 7290-7300.

32. Liu S, Cong Y, Wang D, Sun Y, Deng L, Liu Y, Martin-Trevino R, Shang L, McDermott SP, Landis MD, Hong S, Adams A, D'Angelo R, Ginestier C, Charafe-Jauffret E, Clouthier SG, Birnbaum D, Wong ST, Zhan M, Chang JC, Wicha MS. Breast cancer stem cells transition between epithelial and mesenchymal states reflective of their normal counterparts. Stem Cell Rep, 2014; 2: 78-91.

33. Triscott J, Rose Pambid M, Dunn SE. Concise review: bullseye: targeting cancer stem cells to improve the treatment of gliomas by repurposing disulfiram. Stem Cell, 2015; 33: 1042-1046.

34. Hald J, Jacobsen E. A drug sensitizing the organism to ethyl alcohol. Lancet, 1948; 2: 1001-1004.

35. Conticello C, Martinetti D, Adamo L, Buccheri S, Giuffrida R, Parrinello N, Lombardo L, Anastasi G, Amato G, Cavalli M, Chiarenza A, De Maria R, Giustolisi R, Gulisano M, Di Raimondo F. Disulfiram, an old drug with new potential therapeutic uses for human hematological malignancies. Int J Cancer, 2012; 131: 2197-2203.

36. Iljin K, Ketola K, Vainio P, Halonen P, Kohonen P, Fey V, Grafstrom RC, Perala M, Kallioniemi O. High-Throughput Cell-Based Screening of 4910 Known Drugs and Drug-like Small Molecules Identifies Disulfiram as an Inhibitor of Prostate Cancer Cell Growth. Clinical Cancer Research, 2009; 15: 6070-6078.

37. Yip NC, Fombon IS, Liu P, Brown S, Kannappan V, Armesilla AL, Xu B, Cassidy J, Darling JL, Wang W. Disulfiram modulated ROS–MAPK and NFκB pathways and targeted breast cancer cells with cancer stem cell-like properties. British Journal of Cancer, 2011; 104: 1564-1574.

38. Guo X, Xu B, Pandey S, Goessl E, Brown J, Armesilla AL, Darling JL, Wang W. Disulfiram/copper complex inhibiting NFκB activity and potentiating cytotoxic effect of gemcitabine on colon and breast cancer cell lines. Cancer Letters, 2010; 290: 104-113.

39. Requejo R, Hurd TR, Costa NJ, Murphy MP. Cysteine residues exposed on protein surfaces are the dominant intramitochondral thiol and may protect against oxidative damage. FEBS J, 2010; 277: 1465-1480.

40. Sen, C.K. and Packer, L. Thiol homeostasis and supplements in physical exercise. Am. J. Clin. Nutr, 2000; 72, 653S-669S.

41. Jiao Y, Hannafon BN, Ding WQ. Disulfiram's Anticancer Activity: Evidence and Mechanisms. Anticancer Agents Med Chem, 2016; 16: 1378-1384.

42. Chou TC. Theoretical Basis, Experimental Design, and Computerized Simulation of Synergism and Antagonism in Drug Combination Studies. S Pharmacol Rev, 2006; 58: 621-681.

43. Chou TC, Talalay P. Quantitative analysis of dose-effect relationships: The combined effects of multiple drugs or enzyme inhibitors. Adv Enzyme Regul, 1984; 22: 27-55.

44. Chou TC, Motzer RJ, Tong Y, Bosl GJ. Computerized quantitation of synergism and antagonism of taxol, topotecan, and cisplatin against human teratocarcinoma cell growth: a rational approach to clinical protocol design. J Natl Cancer Inst, 1994; 86: 1517-1524.

45. Irani, K, Xia Y, Zweier JL, Sollott SJ, Der CJ, Fearon ER, Sundaresan M, Finkel T, Goldschmidt-Clermont PJ. Mitogenic signaling mediated by oxidants in Ras-transformed fibroblasts. Science, 1997; 275: 1649-1652.

46. Kincaid MM1, Cooper AA. ERADicate ER stress or die trying. Antioxid Redox Signal, 2007; 9: 2373-2387.

47. Bell, E. L. Chandel, N. S. Mitochondrial oxygen sensing: regulation of hypoxia-inducible factor by mitochondrial generated reactive oxygen species. Essays Biochem, 2007; 43: 17-27.

48. Vurusaner, B., Poli, G. & Basaga, H. Tumor suppressor genes and ROS: complex networks of interactions. Free Radic Biol Med, 2012; 52: 7-18.

49. Meister, A. Glutathione deficiency produced by inhibition of its synthesis, and its reversal; applications in research and therapy. Pharmacol Ther, 1991; 51: 155-194.

50. Bouayed, J. & Bohn, T. Exogenous antioxidants-double-edged swords in cellular redox state: health beneficial effects at physiologic doses versus deleterious effects at high doses. Oxid Med Cell Longev, 2010; 3: 228-237.

51. Chiara Gorrini, Isaac S. Harris and Tak W. Mak. Modulation of oxidative stress as an anticancer strategy. Nature review, 2014; 12:931-947.

52. Tsao, S. M., Yin, M. C., Liu, W. H. Oxidant stress and B vitamins status in patients with non-small cell lung cancer. Nutr Cancer, 2007; 59: 8-13.

53. Patel, B. P, Rawal UM, Dave TK, Rawal RM, Shukla SN, Shah PM, Patel PS. Lipid peroxidation, total antioxidant status, and total thiol levels predict overall survival in patients with oral squamous cell carcinoma. Integr Cancer Ther, 2007; 6: 365-372

54. Brandon, M., Baldi, P. Wallace, D. C. Mitochondrial mutations in cancer. Oncogene, 2006; 25: 4647-4662.

55. Azad, N., Rojanasakul, Y. Vallyathan, V. Inflammation and lung cancer: roles of reactive oxygen/nitrogen species. J. Toxicol. Environ. Health B Crit Rev, 2008; 11: 1-15.

56. Rodrigues, M. S., Reddy, M. M. Sattler, M. Cell cycle regulation by oncogenic tyrosine kinases in myeloid neoplasias: from molecular redox mechanisms to health implications. Antioxid. Redox Signal, 2008; 10: 1813-1848.

57. Cook, JA, Gius D, Wink DA, Krishna MC, Russo A, Mitchell JB. Oxidative stress, redox, and the tumor microenvironment. Semin Radiat Oncol, 2004; 14: 259-266.

58. M. Diehn, R.W. Cho, N. A. Lobo NA, Kalisky T, Dorie MJ, Kulp AN, Qian D, Lam JS, Ailles LE, Wong M, Joshua B, Kaplan MJ Wapnir I, Dirbas FM, Somlo G, Garberoglio C, Paz B, Shen J, Lau SK, Quake SR, Brown JM, Weissman IL, Clarke MF. Association of reactive oxygen species levels and radioresistance in cancer stem cells. Nature, 2009; 458: 780-783.

59. Fei Wang, Shumei Zhai, Xiaojun Liu, Liwen Li, Shirley Wu, Q. Ping Dou, Bing Yan. A novel dithiocarbamate analogue with potentially decreased ALDH inhibition has copper-

dependent proteasome-inhibitory and apoptosis-inducing activity in human breast cancer cells. Cancer Lett, 2011; 300: 87-95.

60. Mauricio Rodriguez-Torres, Alison L. Allan. Aldehyde dehydrogenase as a marker and functional mediator of metastasis in solid tumors. Clin Exp Metastasis, 2016; 33: 97-113.

61. Singh SK, Hawkins C, Clarke ID, Squire JA, Bayani J, Hide T, Henkelman RM, Cusimano MD, Dirks PB. Identification of human brain tumour initiating cells. Nature, 2004; 432: 396-401.

62. Thomas ML, Coyle KM, Sultan M, Vaghar-Kashani A, Marcato P. Chemoresistance in cancer stem cells and strategies to overcome resistance. Chemother Open Access, 2014; 03: 1-10.

63. Santini MT, Rainaldi G, Indovina PL. Multicellular tumour spheroids in radiation biology. Int J Radiat Biol, 1999; 75: 787-799.

64. Liao T, Kaufmann AM, Qian X, Sangvatanakul V, Chen C, Kube T, Zhang G, Albers AE. Susceptibility to cytotoxic T cell lysis of cancer stem cells derived from cervical and head and neck tumor cell lines. J Cancer Res Clin Oncol, 2013; 139: 159-170.

65. Ghods AJ, Irvin D, Liu G, Yuan X, Abdulkadir IR, Tunici P, Konda B, Wachsmann-Hogiu S, Black KL, Yu JS. Spheres isolated from 9L gliosarcoma rat cell line possess chemoresistant and aggressive cancer stem-like cells. Stem Cells, 2007; 25: 1645-1653.

66. Fang D, Nguyen TK, Leishear K, Finko R, Kulp AN, Hotz S, Van Belle PA, Xu X, Elder DE, Herlyn M. A tumorigenic subpopulation with stem cell properties in melanomas. Cancer Res, 2005; 65: 9328-9337.

67. Chen C, Wei Y, Hummel M, Hoffmann TK, Gross M, Kaufmann AM, Albers AE. Evidence for epithelial-mesenchymal transition in cancer stem cells of head and necksquamous cell carcinoma. Plos One, 2011; 6: e16466.

68. He QZ, Luo XZ, Wang K, Zhou Q, Ao H, Yang Y, Li SX, Li Y, Zhu HT, Duan T. Isolation and characterization of cancer stem cells from high-grade serous ovarian carcinomas. Cell Physiol Biochem, 2014; 33: 173-184.

69. He QZ, Luo XZ, Wang K, Zhou Q, Ao H, Yang Y, Li SX, Li Y, Zhu HT, Duan T. Isolation and characterization of cancer stem cells from high-grade serous ovarian carcinomas. Cell Physiol Biochem, 2014; 33: 173-184.

70. Wang F, Zhai S, Liu X, Li L, Wu S, Dou QP, Yan B. A novel dithiocarbamate analogue with potentially decreased ALDH inhibition has copper-dependent proteasome-inhibitory and apoptosis-inducing activity in human breast cancer cells. Cancer Lett, 2011; 300: 87-95.

71. Zhi Guo Zheng, Hong Xu, Sha Sha Suo, Xiao Li Xu, Mao Wei Ni, Lin Hui Gu, Wei Chen, Liang Yan Wang, Ye Zhao, Bing Tian, Yeu Jin Hua. The essential role of H19 contributing to cisplatin resistance by regulating glutathione metabolism in high-grade serous ovarian cancer. Sci Rep, 2016; 6: 26093.

72. Amable L. Cisplatin resistance and opportunities for precision medicine. Pharmacol Res, 2016; 106: 27-36.

73. Dean M, Fojo T, Bates S. Tumour stem cells and drug resistance. Nat Rev Cancer, 2005; 5: 275-284.

74. Tawari PE, Wang Z, Najlah M, Tsang CW, Kannappan V, Liu P, McConville C, He B, Armesilla AL, Wang W. The cytotoxic mechanisms of disulfiram and copper (II) in cancer cells. Toxicol Res, 2015; 4:1439-1442.

75. Song W, Tang Z, Shen N, Yu H, Jia Y, Zhang D, Jiang J, He C, Tian H, Chen X. Combining disulfiram and poly (L-glutamic acid) –cisplatin conjugates for combating cisplatin resistance. Journal of Controlled Release, 2016; 231:94-102.

76. Kim JY, Cho Y, Oh E, Lee N, An H, Sung D, Cho TM, Seo JH. Disulfiram targets cancer stem-like properties and the HER2/Akt signaling pathway in HER2/positive breast cancer. Cancer Lett, 2016; 379: 39-48.

77. N.C. Yip, I.S. Fombon, P.Liu, S.Brown, V,Kannappan, Armesilla, Xu B, Cassidy J, Darling JL, Wang W. Disulfiram modulated ROS-MARK and NF kappa B pathways and targeted breast cancer cells with cancer stem cell-like properties. Br J Cancer, 2011; 104: 1564-1574.

# 8 Curriculum Vitae

My curriculum vitae does not appear in the electronic version of my paper for reasons of data protection.

# 9 Affidavit

“I, [Zhi, Yang] certify under penalty of perjury by my own signature that I have submitted the thesis on the topic [Evaluation of Cytotoxic Effects and Underlying Mechanisms of Disulfiram on Breast Cancer Cell Lines] I wrote this thesis independently and without assistance from third parties, I used no other aids than the listed sources and resources.

All points based literally or in spirit on publications or presentations of other authors are, as such, in proper citations (see "uniform requirements for manuscripts (URM)" the ICMJE www.icmje.org) indicated. The sections on methodology (in particular practical work, laboratory requirements, statistical processing) and results (in particular images, graphics and tables) correspond to the URM (s.o) and are answered by me. My interest in any publications to this dissertation correspond to those that are specified in the following joint declaration with the responsible person and supervisor. All publications resulting from this thesis and which I am author correspond to the URM (see above) and I am solely responsible.

The importance of this affidavit and the criminal consequences of a false affidavit (section 156,161 of the Criminal Code) are known to me and I understand the rights and responsibilities stated therein.

Date Signature

# 10 Acknowledgements

First of all, a special word of thanks to my supervisor Dr. Andreas M. Kaufmann, for offering me the precious opportunity to study at Charité-Universitätsmedizin Berlin, Campus Benjamin Franklin. I consider myself as a very lucky individual to meet him. His patient guidance, kind encouragement and continuous support gave me confidence and helped me to keep on the correct path throughout the entire period of my study. Without his kind direction and proper guidance, this study would have been a little success. I'm using this opportunity to express my deepest gratitude and special thanks to him.

I would like to express my sincere gratitude to Dr. Andreas Albers, who always provided me with professional ideas and suggestions. Although he is quite busy in clinic, he could always take time out to hear, guide, and talk with me. Discussing with him every time helped me with a lot of constructive directions.

I must express my gratitude to Dana Schiller, who gave necessary advice and arranged all facilities in the lab to make life easier. I choose this moment to acknowledge her contribution gratefully.

I would also like to thank all the other members in the lab, Jinfeng Xu, Fang Guo, Weiming Hu, Sarina Sarina, Wenhao Yao, Tina Kube, Amrei Krings, Aleksandra Pesic, Mirka Basten, Nora Franziska Nevermann, Sarah-Maria Klaes, Sarah Thies and all others, for their generous support, coaching and companionship during my whole study in Germany. They shared their expertise with me very generously and I have learnt a lot from them.

I owe my sincere gratitude to my parents, my wife and my son for your love, encouragement and support in every step on my way. You are my sources of power, and made my life full and bright.

I am very grateful to those who helped in any way, your contribution made my study and life full of sunshine. Successfully completion of this project requires helps from a number of persons. As it would be impossible to thank everybody individually, please accept this acknowledgement as an expression of my deepest gratitude. Thank you once again for your great support.